Please cite this article in press as: Shen et al., Designing and integrating microfluidic electrodes for biosensing and micromanipulation, Device (2025), https://doi.org/10.1016/j.device.2025.100964

Device



Review

Designing and integrating microfluidic electrodes for biosensing and micromanipulation

Yigang Shen (沈毅刚),¹ Huaixin Li (李怀鑫),⁴ Ya Li (李亚),⁵ Yingting Wang (王英廷),¹ Kang Chen (陈康),⁵ Jianping Li (李建平),¹ Jijie Ma (马继杰),¹ Song Chen (陈松),¹ Yili Hu (胡意立),¹ Jianming Wen (温建明),¹,⁵,⁵ Xu Hou (侯旭),³,⁴,⁵ and Jin Li (李津)²,⁵

- ¹The Institute of Precision Machinery and Smart Structure, College of Engineering, Zhejiang Normal University, Jinhua, China ²Cardiff School of Engineering, Cardiff University, Cardiff, UK
- ³State Key Laboratory of Physical Chemistry of Solid Surfaces, College of Chemistry and Chemical Engineering, Xiamen University, Xiamen, China
- ⁴Research Institute for Biomimetics and Soft Matter, College of Physical Science and Technology, Xiamen University, Xiamen, China
- ⁵College of Mathematical Medicine, Zhejiang Normal University, Jinhua, China
- *Correspondence: wjming@zjnu.cn (J.W.), houx@xmu.edu.cn (X.H.), lij40@cardiff.ac.uk (J.L.) https://doi.org/10.1016/j.device.2025.100964

THE BIGGER PICTURE Microfluidic chips enable control and measurement of microscale fluids and particles. By integrating different sensing (e.g., electrochemical, impedance, or potential measurement) and manipulation (e.g., electric field, thermal field, magnetic field, or mechanical vibration) functions, microfluidic electrodes transform channels into programmable labs-on-a-chip. Electrodes bridge the electronic and fluidic domains, ultimately determining chip performance. As sensors, they create critical connections between samples in microchannels and external equipment, with their materials and dimensions directly influencing detection resolution, responsiveness, and accuracy. As manipulators, electrodes generate various physical fields through strategic shapes and arrangements, delivering precisely controlled forces at different magnitudes and spatial resolutions, and enabling the accurate manipulation of diverse biological samples. In this review, we detail the working principles and applications of sensing electrodes and micromanipulation electrodes. We propose future development directions regarding manufacturing methods, flexible designs, solid/liquid interface improvements, and the use of AI in design optimization and data analysis.

SUMMARY

Microfluidic systems enable the precise measurement, manipulation, and control of fluids and particles at the microscale, providing new tools and insights for biological, chemical, and medical research. Electrodes are key components of microfluidic systems, functioning both as sensors for target detection and as microactuators for sample manipulation. The integration of functional electrodes into microfluidic devices has broadened the applications of microfluidic technology across various fields, enhancing its capacity to address complex biochemical challenges. In this review, we first examine the construction of microfluidic electrodes, focusing on manufacturing and bonding methods. We then classify the electrodes into two classes, i.e., sensing and manipulation, and discuss their fundamental principles alongside representative real-world applications. Finally, we highlight current challenges in microfluidic electrode technology and propose innovative design strategies for electrode integration that could stimulate new research into micro/nano fabrication, chemical engineering, and biological engineering.

INTRODUCTION

Integrated microfluidic systems allow for the integration of various functional units on a single platform, enabling multiple tasks to be performed in parallel. In combination with advancements in microelectromechanical systems (MEMSs) and nanotechnology, integrated microfluidic systems can help in analyzing chemical and biological samples. These systems facilitate the detection of target species, separation of mixtures,

sample purification, and synthesis of new materials. An integrated microfluidic system typically includes microfluidic channels, valves, pumps, mixers, and electrodes. Electrodes are used to establish electrical contact with the fluid and to generate electric, thermal, acoustic, and magnetic fields that can be employed to sense and manipulate fluids and particles. The performance and configuration of electrodes directly influence the sensitivity of detection and analysis, the integrity and reliability of sensing signals, and the accuracy of manipulations.



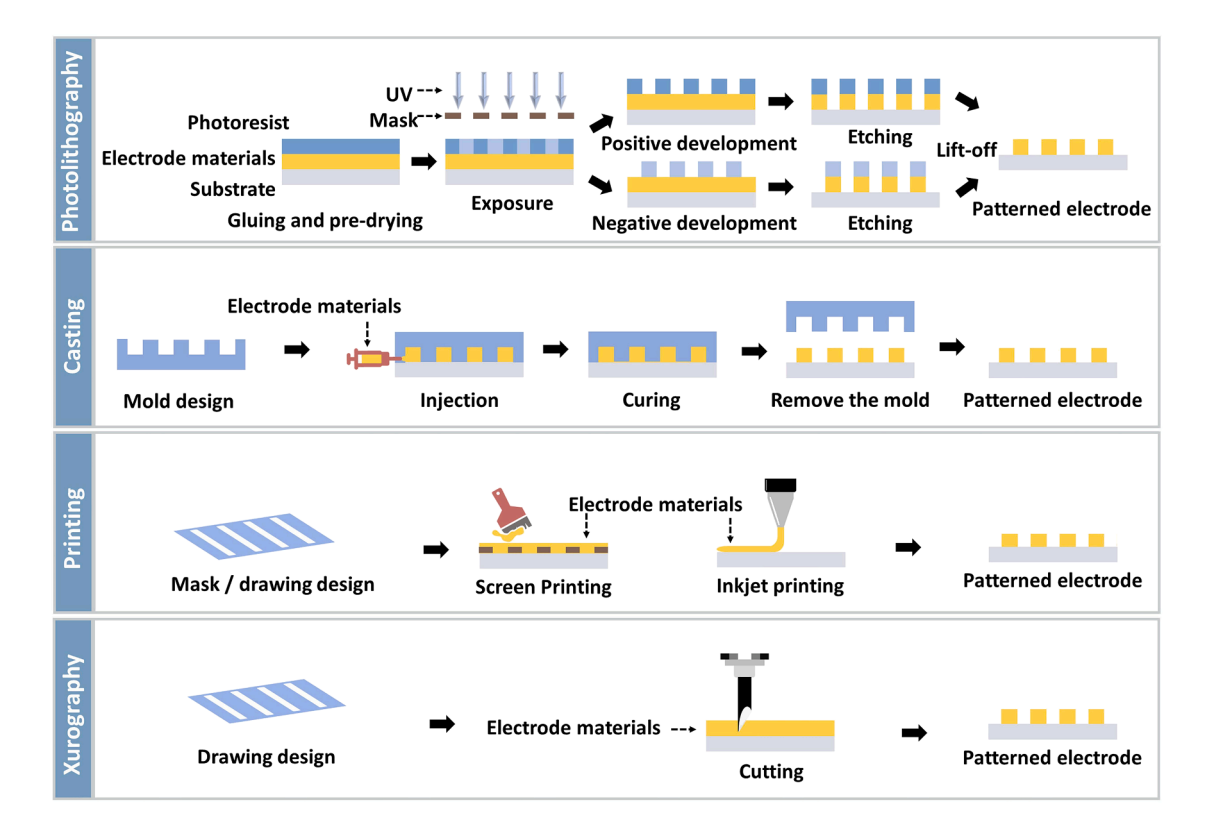


Figure 1. Flow diagrams of the commonly used microfluidic electrode manufacturing processes From top to bottom: photolithography, casting, printing, and xurography.

Over the years, microfluidic systems have evolved from basic chemical analysis applications to droplet microfluidics for single-cell analysis and, most recently, to organ-on-a-chip technology, which is a microfluidic cell-culture platform that re-creates key structural and biochemical features of living tissues.²

Previous reviews have discussed the principles and applications of integrated microfluidics, such as in dielectrophoresis (DEP),³ DNA analysis,⁴ and wearable devices.⁵ In this review, we focus on the perspectives of electrode fabrication and bonding techniques and the development of sensing electrodes and manipulation electrodes. We classify electrodes based on their functions and discuss their basic operating principles and recent developments. We also discuss remaining challenges and outline future directions for microfluidic electrode fabrication and applications.

FABRICATION TECHNIQUES OF MICROFLUIDIC ELECTRODES

In the context of MEMS and microfluidics, electrodes are essential for establishing electrical contact between biological samples and the sensing/control devices. Electrodes inject electric current into the fluid, creating an electric field that can be harnessed for sensing and manipulating fluids or particles. Figure S1 shows an overview of these advancements in both microfluidics and electrode technology. In the design of electromicrofluidic chips, the fabrication of electrodes and the bonding

methods used to integrate electrodes with microchannels are chosen based on the intended functionalities, and the choice of electrode materials often determines which manufacturing methods are applicable. Researchers frequently use one or a combination of these techniques to produce electrodes with the desired properties. In this section, we introduce several widely used fabrication and bonding methods for integrating electrodes into microfluidic systems.

Photolithography and etching

Photolithography is a technique for transferring a predefined pattern from a mask onto a substrate coated with photoresist by selectively removing parts of the substrate surface. It generally involves five steps: (1) photoresist coating, (2) UV exposure, (3) development, (4) etching, and (5) photoresist removal (liftoff) (see Figure 1). The technique offers several advantages for fabricating microfluidic electrodes: (1) precision and resolution reaching the nanometer scale; (2) complex patterning, enabling intricate two- (2D) and three-dimensional (3D) structures; (3) repeatability and consistency suitable for mass production; (4) flexible and customizable design enabling diverse functionalities; and (5) strong compatibility for integrating with other microfabrication technologies (e.g., microfluidic channel manufacturing).

While photolithography is a mature micro/nanofabrication method, its chemical processes can damage the layers and interfaces in the finished device. In many microsystems, patterning





occurs directly on solvent-susceptible organic functional layers (e.g., conjugated polymers, small-molecule organics, or bioactive coatings). Standard resists/developers (e.g., propylene glycol methyl ether acetate (PGMEA) or aromatic solvents) and UV/bake steps can dissolve, dope, or oxidize these layers, degrading device performance, although in some cases, an orthogonal photoresist/solvent can be used to mitigate such damage. Additionally, photoresist residues and photoacidgenerator by-products can remain after processing, affecting downstream wetting, protein adsorption, and cell viability. Elastomeric substrates such as polydimethylsiloxane (PDMS) also readily absorb common lithographic solvents, causing swelling, feature distortion, and subsequent leaching into microchannels during biological operations.

Casting

Casting offers an alternative when direct contact with lithographic solvents, resist residues, and PDMS swelling are of concern. This technique can form electrodes without exposing solvent-sensitive layers or biotic interfaces to photoresists/developers. In the casting approach, conductive materials (e.g., liquid metals [LMs], inks, or conductive polymers) are introduced into prefabricated molds and then solidified under specific conditions (e.g., temperature, pressure, or atmosphere). After curing, the mold is removed, leaving behind the desired electrode (Figure 1). Casting addresses some of the drawbacks of photolithography, such as mold-limited resolution/roughness, linewidth floors set by filling and trapped air, shrinkage/warpage and adhesion issues during curing, material constraints, and restricted multi-layer alignment. Nevertheless, photolithography remains preferred for sub-10-μm, wafer-scale uniformity, whereas casting excels in rapid, mask-free prototyping and thick/3D electrodes on soft substrates.8,9

Screen printing, inkjet printing, and 3D printing

Screen-printing technology is widely used in circuit board manufacturing. In this method, conductive ink is transferred through a patterned screen, producing the desired electrode shape once the ink dries (Figure 1). A critical step in screen printing is designing and preparing the printing plate, typically achieved by coating a polyester or stainless-steel mesh with a photographic emulsion and exposing it through a photomask to define the open areas. 10 The conductive ink typically consists of carbon, silver, gold, platinum, or copper powders, along with additives such as thickeners. Screen printing provides cost-effective design flexibility with \$10-\$100 reusable stencils and high productivity through automated lines producing hundreds of prints hourly. 11 It creates 5- to 50-μm-thick films with linewidths of 50-100 μm, making it ideal for large-area, low-cost production. 12 Compared to photolithography, screen printing offers lower resolution and alignment accuracy. Achieving features smaller than 20 µm and wafer-scale alignment remains impractical with conventional screens. Quality improvements come from controlling emulsion-over-mesh processes, optimizing squeegee parameters, and using thermal/photonic sintering. Surface contamination can affect analysis, but low-residue inks and standardized procedures enhance detection precision. 13,14

Inkjet printing is a non-contact method for fabricating electrodes that does not require a lithography mask (Figure 1). In this process, a computer-controlled nozzle deposits different inks directly onto the substrate to form the designed electrode patterns. 15 Printable inks typically have viscosity of \sim 5–20 mPa·s and surface tension of ~25-50 mN·m⁻¹, requiring water-based systems to include dispersants, humectants, and surfactants. 16,17 Under optimal conditions, inkjet produces $\sim\!20$ - to 50-µm linewidths (with ${\sim}50\text{--}100~\mu\text{m}$ being practical for robust devices), while aerosol jets can achieve \sim 10 μm at lower area throughput. 16 The main advantages of inkjet printing include a maskless process and easy design iteration. However, this method faces limitations, including nozzle clogging, coffee-ring formation, and post-print sintering requirements. Due to the limited nozzle size, particles in the ink can easily clog the nozzle. Studies recommend particles of <200 nm (less than 1/10 of nozzle size) to prevent clogging. 18 The coffee-ring effect causes uneven distribution of solid particles on the substrate after ink drying, resulting in electrode quality issues. The coffee-ring effect can be suppressed by inducing Marangoni flows, which describe the surface-tension-driven circulation caused by composition/temperature gradients. Using binary solvents such as a fast-evaporating low-surface-tension component with a slower, higher-surface-tension cosolvent or mild substrate heating creates a surface tension gradient that drives inward surface flow. This flow counteracts the outward capillary flux, resulting in more uniform electrode films. 19,20 Environmental humidity also influences deposition patterns. A highly controlled humidity environment during printing increases electrode quality and reproducibility. For densification, chemically reactive silver inks are effective at low temperatures, with particle-free Ag precursor inks achieving high conductivity at room temperature and near bulk-Ag conductivity after mild annealing at 90°C.^{21,22}

Three-dimensional printing enables the fabrication of electrodes with high precision and complex geometries by depositing materials layer by layer under digital control. Compared to subtractive processes (e.g., lithography and milling), this additive approach generates minimal waste, thereby reducing costs associated with raw materials, storage, and energy consumption. For a given design, 3D printing can produce an object and allow for straightforward iterations, potentially shortening the R&D cycle.²³ Based on bonding mechanisms and material types, common 3D printing methods include material extrusion (e.g., fused deposition modeling, direct ink writing, and robocasting), vat photopolymerization (e.g., stereolithography [SLA] and digital light processing [DLP]), powder bed fusion (e.g., metal laser sintering and electron beam melting), material jetting, sheet lamination, and directed energy deposition (e.g., laser-engineered net shaping).^{24,25} Three-dimensional printed electrode materials face a trade-off between printability and conductivity. Inks and filaments require binders or solvents to be printable, while high conductivity necessitates dense metal networks that typically demand post-processing methods such as laser sintering or electroplating.²⁶ Photocured resins remain largely non-conductive even with added conductive fillers (e.g., a DLP acrylate with 4.8 wt % polyaniline reached only $\sim 10^{-3}$ S cm⁻¹).²⁷ Extruded composites conduct electricity much worse than electroplated metals and tend to crack under stress (e.g.,





commercial black carbon/graphite filaments show bulk resistivities of $\sim\!\!3.9\text{--}27~\Omega\cdot\!\text{cm}$ and increased brittleness with higher filler content). Biocompatibility issues stem from residual monomers/photoinitiators and from metal-ion leaching. SLA parts release chemicals that can reduce cell viability without additional treatment. In summary, while 3D-printed electrode structures offer speed and design flexibility, they require additional processing to meet the performance standards of microfluidic devices.

Xurography

Xurography, also known as craft cutting/writing or razor writing, was first introduced as a micromachining technique that uses physical blades to pattern various materials (e.g., polymer films, metal foils, or paper). 30 Xurography does not require a clean room and avoids the burning marks associated with laser cutting. By integrating with computer-aided design (CAD) software, xurography can also be used to produce masks for different applications (e.g., electrode sputtering, electroplating, and wet chemical etching) and to create microfluidic channels. By slicing through multiple stacked layers, xurography facilitates the simultaneous fabrication of numerous microfluidic electrodes and layered composites. However, it is unsuitable for cutting thicker, harder materials and is limited by its relatively low resolution. Kongkaew et al. demonstrated a craft-and-stick xurography workflow that uses cut graphene-paper electrodes and polyethylene terephthalate (PET) microfluidic layers to create a flexible electrochemical platform.31 When functionalized with Prussian blue and glucose oxidase, the device provides reliable glucose sensing. Wu et al. demonstrated an AC-electroosmosis micromixer device by using the xurography method.³² Biocompatible adhesive and copper foil are prepared with a digital cutting plotter and laminated to create channels with tooth-shaped electrodes. Their work highlights the value of xurography in developing disposable biosensors and point-of-care diagnostic tools.

Other fabrication methods and bonding techniques

Beyond conventional methods, several novel and portable approaches have been developed for fabricating electrodes in microfluidic systems. For example, growing specific particle composites on a solid contact (SC) can yield sensing electrodes. Huang and colleagues modified gold surfaces with wrinkled microspheres composed of graphene oxide (GO) and zeolitic imidazolate framework (ZIF-8) composites, demonstrating highly sensitive responses to inorganic salt ions.³³ As another example, Economou and coworkers used a pen-on-paper plotting approach to fabricate multiple paper-based glucose detection array electrodes in a single batch.³⁴ Other techniques, such as transfer printing, dealloying, and wire integration, can also be integrated into the electrode fabrication process. Transfer printing enables patterning of conductive features onto elastomers without exposing solvent-sensitive layers. For example, tape transfer of Galinstan onto semi-cured PDMS produces ~150μm lines that support stretchable circuits. 35 Dealloying of Ag-Au creates nanoporous gold electrodes with a high surface area and excellent biofouling resistance; however, designers must account for material shrinkage and mechanical fragility during the process.³⁶ Another approach, wire integration, involves directly inserting microwires into elastomer devices. Douville et al. embedded Ag/AgCl wire electrodes in two-layer PDMS surrounding a porous membrane (500-μm Ag/AgCl wires seated in 500-μm grooves), enabling robust, deposition-free measurements inside the microchannel.³⁷

When one is designing electrodes for different functions, materials must be chosen to ensure electrical conductivity, chemical stability, and biocompatibility. Gold and platinum are the most widely used electrode materials due to their conductivity and inertness, although their high cost restricts broader application. Silver, while more conductive and less expensive than gold and platinum, lacks chemical stability. Carbon, by contrast, offers conductivity, chemical stability, and low cost, making it a viable alternative. However, the choice of carbon materials also has limitations. Carbon films have conductivity several orders of magnitude lower than metals, which increases series resistance and noise; carbon surfaces are easily contaminated in complex media, thus requiring surface treatment or antifouling coatings; and because carbon cannot be soldered, establishing reliable interconnections with external wires presents challenges. Other materials, such as liquid metals and conductive polymers, have been investigated for microfluidic electrodes, each offering benefits, including reduced cost, flexibility, and biocompatibility. Table S1 summarizes the characteristics of various electrode materials and the corresponding fabrication methods.

After fabrication, the electrodes must be bonded with microchannels to form enclosed devices. Thermal bonding is a temperature-driven direct bonding method commonly employed for thermoplastic materials like polycarbonate (PC), PDMS, polymethyl methacrylate (PMMA), and nylon. The materials are heated to their glass-transition temperature, and pressure is applied to ensure tight contact, promoting the diffusion of polymer chains across the surfaces and forming a robust bond upon cooling. However, bubble formation between heated layers can deform the channels.³⁸

Solvent bonding is a direct bonding approach used for layers of polymer materials with identical compositions. Solvents such as ethanol and cyclohexane temporarily soften and dissolve portions of the polymer layers, facilitating the interlinking of polymer networks. The bonding effect is realized after the solvent evaporates. Although solvent bonding minimizes channel deformation, the introduction of organic solvents can reduce device biocompatibility.

Another direct bonding method is oxygen plasma surface treatment, often used for bonding PDMS microchannels. Activated PDMS surfaces expose numerous silanol (-Si-OH) groups, which can form covalent siloxane (-Si-O-Si-) bonds between layers, resulting in irreversible bonding. However, this method provides limited bonding strength for other materials, such as polystyrene (PS). Additionally, corona treatment and UV/ozone treatment are frequently used for surface activation bonding. Table S2 summarizes the characteristics of these bonding methods.

Adhesive bonding is an indirect bonding technique that applies adhesives (e.g., epoxy resin or silicone-based adhesives) or intermediary layers (e.g., double-sided tape or pressure-sensitive adhesives) between surfaces. Although it is cost effective,





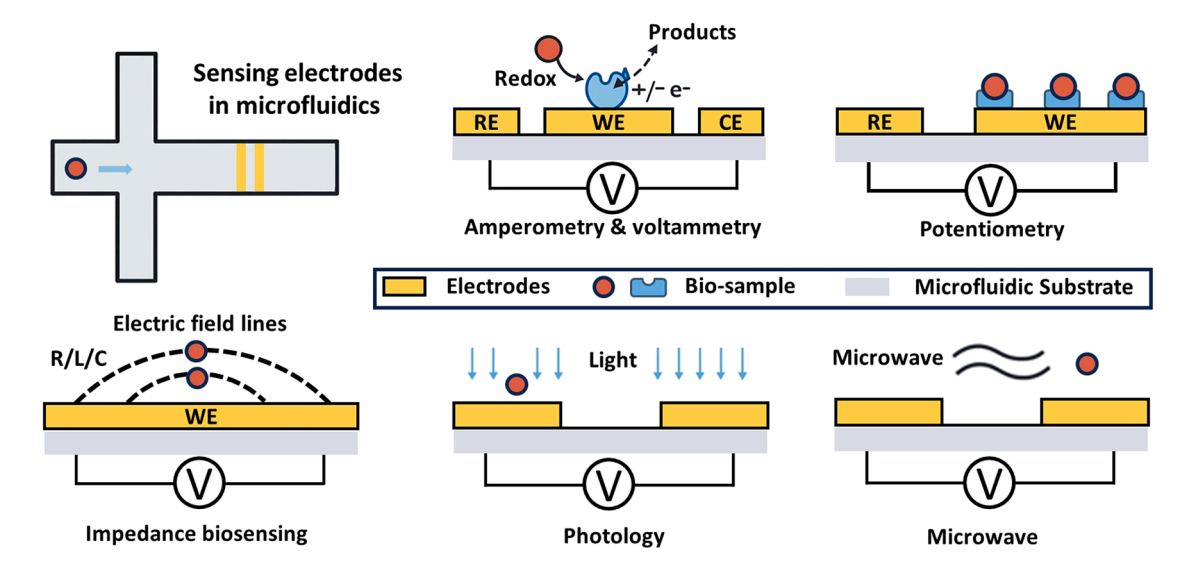


Figure 2. Illustration of various sensing technologies by electrodes in microfluidics: Amperometry and voltammetry, potentiometry, impedance biosensing, photology, and microwave

simple, and fast, drawbacks include adhesive residue, biocompatibility concerns, and relatively lower bonding strength. ⁴⁰ Other bonding strategies include magnetic bonding, surface micro/nano-shape bonding, and vacuum reversible bonding. ⁴¹

SENSING ELECTRODES

Sensing electrode units convert physical and chemical signals from a sample into recognizable electrical signals. Here, we categorize microfluidic electrode signals into three types based on their readout methods: electrochemical current signal modalities, optical signal modalities, and microwave signal modalities (Figure 2).

Electrochemical current signal modalities

In microfluidic electrode devices, electrochemical readouts convert local chemical events into electrical signals with high spatiotemporal resolution. An electrochemical system within a microfluidic chip includes a working electrode (WE), a reference electrode (RE), and a counter electrode (CE). Three key signal modalities are used: current-based methods (amperometry at fixed potential or voltammetry with varying potential) quantify redox analytes and enzyme reporters; potential-based methods (potentiometry) measure the open-circuit potential between the WE and the RE without externally applied current, using high input impedance to keep interelectrode currents at pA-fA levels; and impedance-based methods, such as electrochemical impedance spectroscopy (EIS) and impedance flow cytometry (IFC), examine interfacial and tissue/barrier properties across ~10 Hz-100 kHz for cell monitoring.

Amperometry and voltammetry

Electrochemical current analysis applies a potential to the WE and measures the resulting current, which reflects the extent of oxidation or reduction of the target analyte. In amperometry, a constant potential applied to the WE yields a steady-state

current proportional to analyte concentration, enabling direct quantification of redox activity. Representative techniques include chronoamperometry and rotating disk electrode methods. 42,43 Voltammetry, by contrast, applies a programmed scanning potential (e.g., linear, pulse, or cyclic waveform) to the WE, capturing the dynamic current-potential relationship. This approach measures the analyte concentration and provides mechanistic insights, such as reaction reversibility and adsorption behavior. Examples include cyclic voltammetry, differential pulse voltammetry, and stripping voltammetry. Both amperometry and voltammetry rely on a three-electrode configuration to maintain precise potential control: the WE for target recognition, the RE for potential stability, and the CE to close the electrical circuit.

Amperometric and voltammetric sensing electrodes have been developed for point-of-care testing (POCT), wearable devices, and implantable devices. Zhang and colleagues employed micropillar array electrodes that disrupt microfluidic flow while leveraging MXene fiber-gold nanoparticle 3D structures to enhance electrolyte transport, enabling efficient alphafetoprotein detection.44 Researchers have worked on the miniaturization and integration of these detection technologies. For instance, Liu and coworkers combined origami design with amperometric sensing to develop a portable microfluidic paper-based device (µPAD) for diagnosis of three cardiac blood proteins, aiding early cardiovascular disease prevention (Figure 3A).⁴⁵ These detection methods can be incorporated into wearable devices for analyzing target substances in bodily fluids, particularly sweat. Wang and coworkers described a wearable chip featuring patterned metal electrodes and phenylalanine-imprinted enzyme-mimicking molecularly imprinted polymers (MIPs) capable of direct electrocatalytic oxidation of phenylalanine, achieving high sensitivity and specificity for sweat analysis (Figure 3B).46 Integrating wireless data transmission can enable real-time health monitoring and timely alerts. For



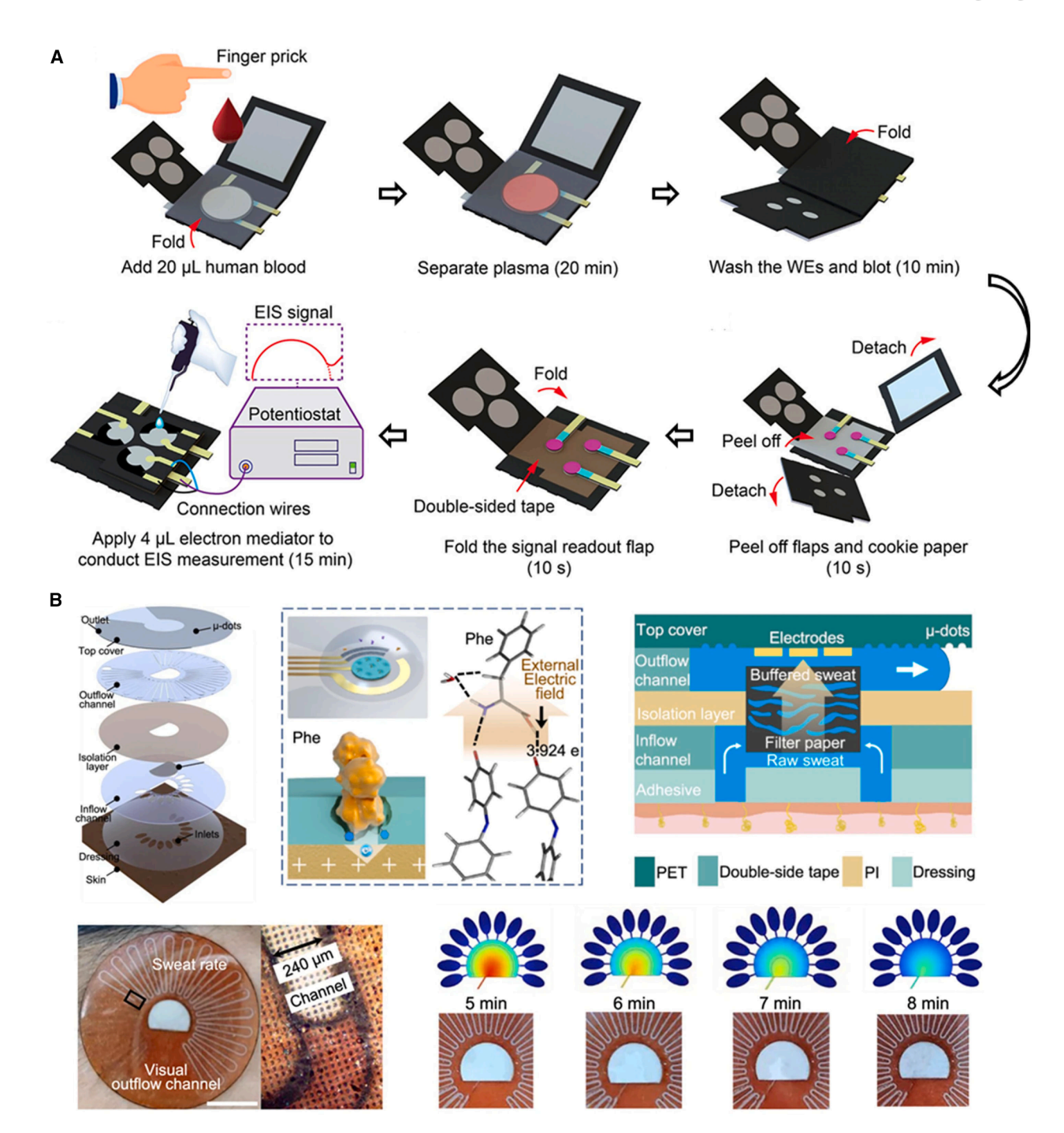


Figure 3. Microfluidic systems with sensing electrochemical electrodes for amperometry and voltammetry

(A) Schematics of an electrochemical μPAD (E-μPAD) featuring an all-in-one origami design for rapid detection of cardiac protein markers in whole blood. E-μPAD protocol for cardiac marker detection from finger-prick blood (copyright 2023, American Chemical Society). 45

(B) Layered structure of a wearable microfluidic chip with integrated sensing electrodes for sweat analysis. The electrodes detect sweat Phe through direct electrocatalytic oxidation, with theoretical simulation showing charge transfer between the electrode and the Phe molecule under an external electric field. Working principle of the vertically assembled microfluidic module. Photographs of the device during exercise on skin and optical micrographs of sweat flow, alongside comparative analysis of simulated predictions versus experimental observations of sweat sampling and filling. Scale bar, 1 cm (copyright 2024, Springer Nature).





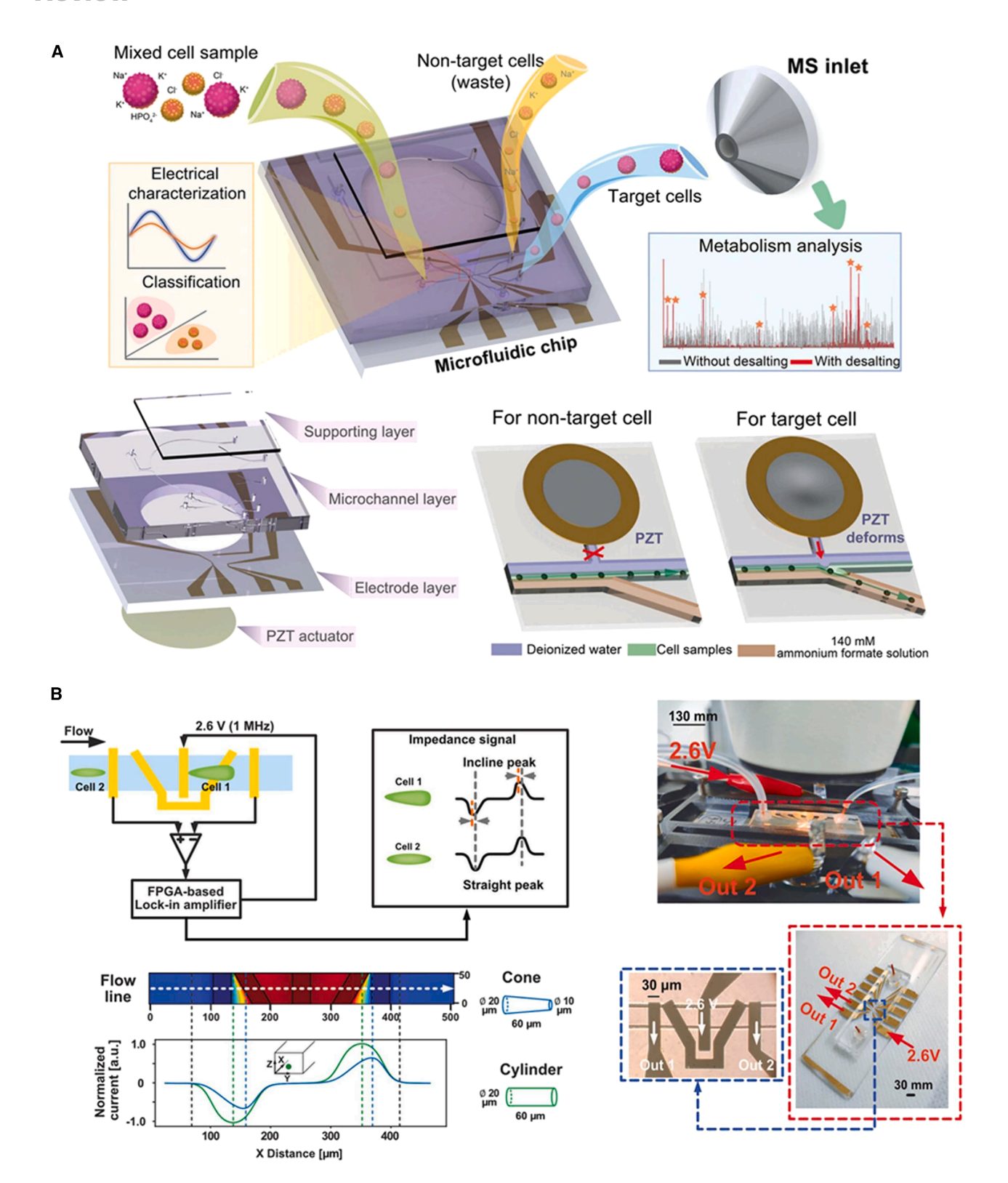


Figure 4. Microfluidic systems with sensing electrochemical electrodes for impedance biosensing

(A) Schematics of impedance flow cytometry-based single-cell sorting and desalting for mass spectrometry (MS) analysis. Layered structure of the microfluidic chip: supporting layer, microchannel layer, electrode layer, and PZT actuator. Operating principle of PZT-based simultaneous sorting and desalting for single cells (copyright 2024, Wiley).⁵⁷

(legend continued on next page)





example, Liu et al. used screen-printed carbon conductive ink for the WE and the CE and Ag/AgCl conductive ink for the RE, followed by electrochemical deposition to measure riboflavin and pH in sweat, with the results wirelessly transmitted for real-time nutritional health tracking.⁴⁷

Potentiometry

Potentiometry uses a two-electrode system, consisting of a WE and an RE, to measure target species by detecting the potential difference arising from surface charge changes when the target species binds on the sensing electrodes. Potentiometric systems employ ion-selective electrodes (ISEs) composed of ion-selective membranes and a liquid contact structure. Based on the membrane material, ISEs can be classified into glass membrane electrodes, liquid electrodes, and solid electrodes. Solid and liquid electrodes, in particular, can be integrated into clinical analysis platforms for applications such as blood analysis, enzyme reaction measurements, nucleic acids assay, and proteins detection. ⁴⁸

Papautsky and colleagues combined SC ISEs (SCISEs) with electronic and fluidic components to develop a self-calibrating system capable of multiplexed ionic analyte sensing. 49 Potentiometry detection methods can be incorporated into wearable devices for sweat analysis. For instance, Liu and coworkers developed a sandwich-type microfluidic patch featuring annular copper electrodes that measured sweat rate and sweat chloride concentration by tracking changes in double-layer capacitance and charge-transfer resistance.⁵⁰ Woon-Hong Yeo and colleagues integrated three ISEs with flexible circuitry to design a saliva electrolyte sensing system, serving as a non-invasive platform for continuous, real-time monitoring of an infant's health condition.⁵¹ Additionally, industrial water quality detection and treatment are also important application areas for potentiometric methods. Xu et al. fabricated all-solid-state ISEs using copper and conductive polymers (poly(3,4-ethylenedioxythiophene) and polystyrene sulfonate [PEDOT/PSS]) via electrodeposition. They optimized a copper-ion-selective membrane and incorporated it into a microfluidic chip, enabling precise boiler water quality detection.52

Impedance-based techniques

Impedance spectroscopy is a label-free, non-destructive, and real-time detection method that measures impedance signals at the electrode-solution interface to characterize the properties of samples in microfluidic channels. To achieve high-precision impedance measurements, electrodes are generally integrated into these channels. When an AC voltage is applied, factors such as the electrode geometry, the fluid's conductivity and dielectric properties, and the presence of charged substances influence the impedance measurement. By analyzing the resulting impedance spectrum, researchers can obtain information about the fluid's properties and composition, and the presence of target species can be obtained. 53

Using electrical impedance spectroscopy, Queirós and colleagues achieved sensitive and quantitative detection of

surfactant protein B (SPB) in amniotic fluid on a screen-printed gold electrode modified through surface functionalization, with a detection limit of 0.1 ng/mL. The electrochemical biosensor for SPB detection can provide benefits for prophylaxis and treatment of neonatal respiratory issues. ⁵⁴ Researchers design complex, 3D topological or patterned electrodes to increase the mass-transfer interface area, thus enhancing detection sensitivity. Hallaj and coworkers demonstrated this approach by leveraging the electrocatalytic properties of paper-based microfluidic electrodes composed of Ni/Fe layered double hydroxide for SARS-CoV-2 antigen detection. ⁵⁵ Their large surface area, adjustable pore sizes, and mass transfer topology produced strong electrical signals, elevating detection sensitivity.

In addition to the impedance analysis methods discussed earlier, which are based on chemical reactions, IFC can provide label-free characterization of biological cells. ⁵⁶ In IFC, a liquid containing particles or cells is continuously injected so that they flow through a set of detection electrodes. By simultaneously measuring changes in current as particles pass through at multiple frequencies, the technique can detect differences in cell shape, structure, and composition. Leveraging the fluid-handling capabilities of microfluidic systems and their multi-channel parallel design, IFC enables high-throughput, high-precision biological detection.

Wang and colleagues employed the IFC framework and piezoelectric transducers (PZTs) in a microfluidic chip to sort breast cancer cells and desalinate solutions, mitigating the impact of non-volatile salts on the generation of single-cell mass spectrometry (Figure 4A).⁵⁷ This detection method can collect chemical information from cells and physical information such as the 3D shape of single cells. Yalikun and coworkers found that asymmetric cells passing through customized electrodes produced asymmetric impedance signals with unequal slopes and peaks, which differed from the signal of a symmetric cell. They proposed a quantitative tilt index to assess the degree of cell asymmetry and demonstrated that this index is independent of the cell's movement trajectory, providing insights into singlecell shape measurement (Figure 4B).⁵⁸

Optical signal modalities

Photology detects molecular interactions by assessing changes in optical properties (such as intensity, wavelength, refractive index, or polarization) caused by the binding of target molecules to the sensing electrode surface. In optical biosensors, electrodes are used to immobilize specific molecules and function both as recognition elements and as transmitters of optical signals. Common types of optical biosensors include surface plasmon resonance (SPR) sensors and silicon photonic (SiP) sensors.

In SPR sensors, the electrode surface is coated with functional molecules that recognize specific analytes. When target substances bind to these molecules, the oscillation behavior of the plasmons at the metal-dielectric interface changes, altering the refractive index and reflectivity of the incident light. This shift

⁽B) Microscopic impedance cytometry for single-cell shape quantification. Schematics of the microfluidic system with multiple electrodes for single-cell shape measurement. The integrated device consists of a PDMS block incorporating microfluidic channels with inlet/outlet ports permanently bonded to a borosilicate glass substrate patterned with Cr/Au electrodes. Simulated impedance results for symmetric and asymmetric micro-objects in microchannels (copyright 2021, Elsevier). Second control of the microfluidic system with multiple electrodes for single-cell shape measurement. The integrated device consists of a PDMS block incorporating microfluidic channels with inlet/outlet ports permanently bonded to a borosilicate glass substrate patterned with Cr/Au electrodes. Simulated impedance results for symmetric and asymmetric micro-objects in microchannels (copyright 2021, Elsevier).





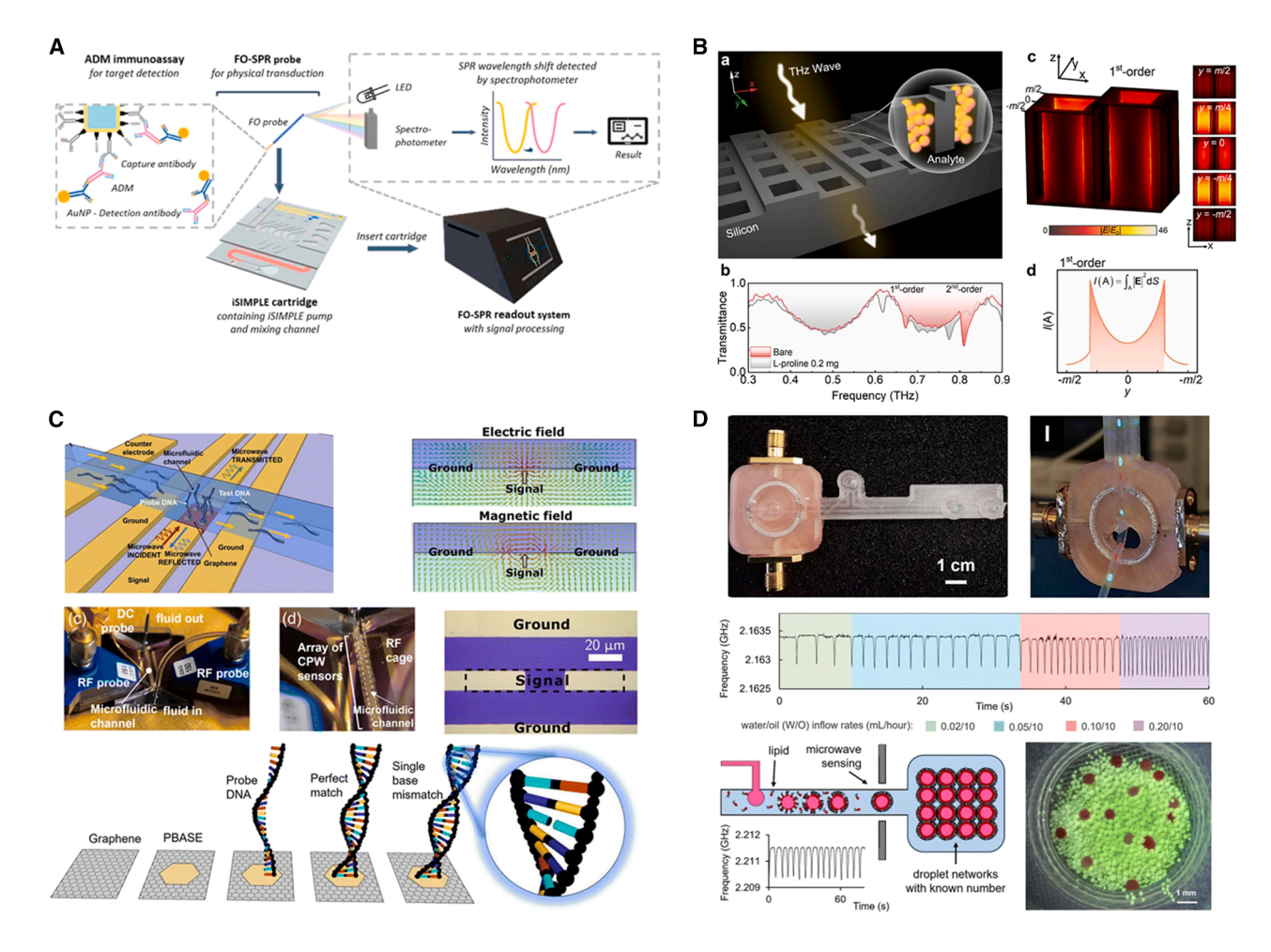


Figure 5. Microfluidic systems with sensing electrodes for photonic and microwave technologies

(A) A plasma detector based on fiber surface plasmon resonance combined with microfluidics. Detection via a one-step adalimumab (ADM) immunoassay on the functionalized fiber optic (FO) probe, analyzed by an FO-SPR portable system (copyright 2022, Elsevier). 60

- (B) An all-dielectric metamaterial sensor for passive trapping. THz transmittance comparison with 0.2 mg L-proline, supported by electric field simulations (copyright 2024, Elsevier).⁶¹
- (C) A graphene-based wideband microwave sensor within microfluidics for DNA recognition. Coplanar waveguide analysis with signal conductor and DNA detection (copyright 2023, The Royal Society of Chemistry). 62
- (D) A 3D-printed microwave-microfluidic device with liquid metal electrodes. Formation and microwave characterization of droplet networks, monitored in flow and assembled into droplet interface bilayer networks (copyright 2024, The Royal Society of Chemistry). 63

provides biological information in the spectrum.⁵⁹ Lammertyn and coworkers combined a fiber-optic SPR sensor with self-powered microfluidics to enable portable detection of adalimumab in plasma,⁶⁰ achieving a detection limit of 0.35 μg/mL (Figure 5A). SiP sensors use silicon or silicon nitride waveguides to confine near-infrared light in both vertical and horizontal dimensions. Part of the electric field extends beyond the waveguide as an evanescent field, interacting with the surrounding medium to form a region sensitive to refractive-index changes. An all-silicon dielectric metamaterial sensor featuring etched grooves and hole arrays can passively capture biomolecules in its resonant cavity via an electric field, promoting light-matter interactions.⁶¹ This design enables qualitative and quantitative analysis of different amino acids, filling a gap in terahertz sensor research (Figure 5B).

Microwave signal modalities

Microwave-based microfluidic biosensors can be classified into narrowband sensors, which detect resonance shifts, and broadband sensors, which extract complex permittivity. Liu and colleagues integrated metamaterials into the microwave sensor fabrication, designing an ultrasmall ($20 \times 16 \text{ mm}^2$) device composed of a square split-ring resonator and a microstrip transmission line. This sensor detects the concentration of substances by analyzing their dielectric constants, achieving a maximum deviation of less than 0.7%, which can be used for medical diagnostic tools and environmental detection methods. Lombardo and coworkers coupled gated graphene waveguides with microfluidic channels to create a sensor that leverages the dual mechanism of dynamic conductivity modulation from chemical electrostatic doping in graphene and wave-propagation changes





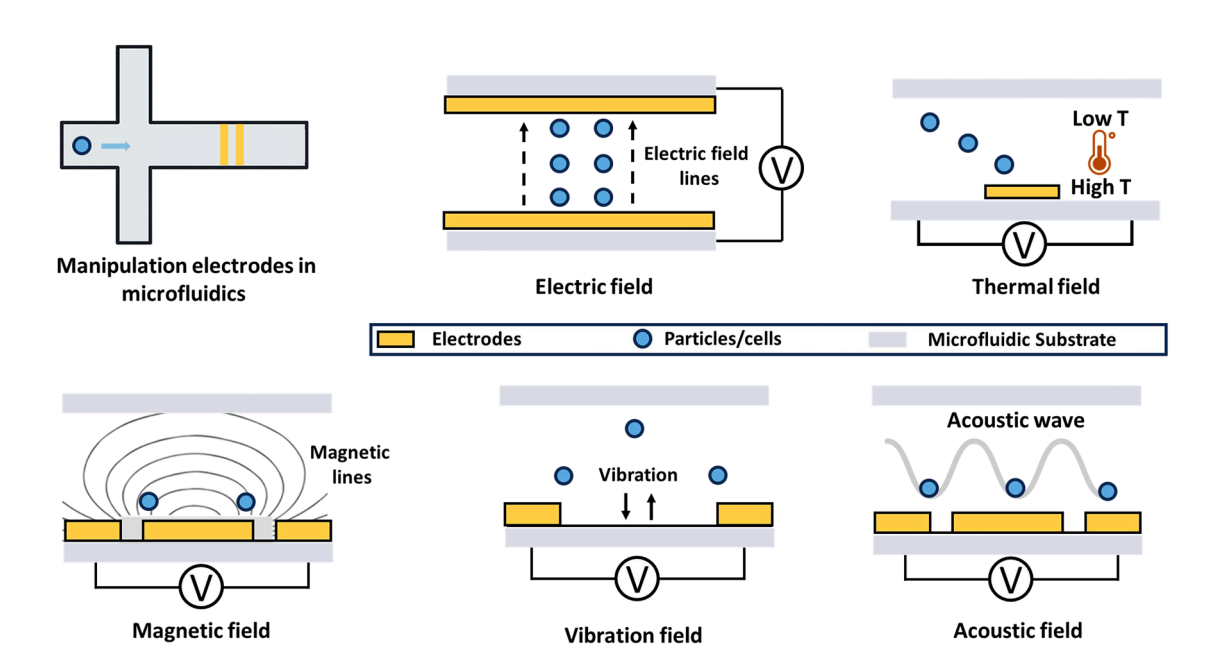


Figure 6. Illustration of various manipulation electrodes in microfluidics: Electric field, thermal field, magnetic field, vibration field, and acoustic field

induced by edge field interactions with analytes. ⁶² It can analyze DNA sequences, offering sensitivity beyond that of field-effect transistors and single microwave sensors in detecting single-base mismatches (Figure 5C). Three-dimensional print technology and the use of liquid metal have enhanced microwaves within microfluidic systems, making them more integrated and portable. For instance, Li and coworkers presented a 3D-printed microfluidic chip incorporating liquid-metal electrodes as microwave splitring resonators to generate and detect water in oil emulsions (Figure 5D). ⁶³ These emulsions could form a droplet network, which acquired functionality via artificial cellular membranes and reagents contained within each droplet component, exemplifying applications in cell-free expression and synthesis. ^{65,66}

Compared to electrochemical analysis, physical analysis methods such as impedance-based and optical techniques can detect target substances without chemical reactions. This non-destructive nature allows for repeated measurements or further analyses on the same sample, a crucial advantage in areas such as drug development and quality control. Additionally, other physical properties, such as flow rate and temperature, can be obtained by direct measurements with electrodes, further expanding the capabilities of these methods.

MANIPULATION ELECTRODES

Manipulation electrodes can generate electrical, thermal, magnetic, and mechanical forces, all of which are essential for controlling fluids and particles within the system (Figure 6).

Electric field

Electric fields in fluids can induce electrodynamic phenomena such as electrophoresis and electroosmosis. Electrophoresis leverages these fields to separate various biological samples, e.g., nucleic acids, molecules, urine, and cell lysates, based on differences in charge and size, whereas electroosmosis involves fluid flow driven by the motion of charged particles in response to the electric field. These mechanisms are vital for tasks in analytical and diagnostic applications, including sample preparation, mixing, and separation.⁶⁷

An electrokinetic microfluidic system typically requires two electrodes embedded in the inlet and outlet of the microchannels. For example, Ramachandran et al. used isotachophoresis in a microfluidic device to detect SARS-CoV-2 in 35 min with high sensitivity and specificity⁶⁸ (Figure 7A). An electric field can also enable the manipulation of biological entities, e.g., cells and DNA, through DEP, which uses non-uniform fields to exert forces on dielectric particles. This approach is useful for applications such as cellular assays and tissue engineering, where non-contact cell handling is essential. In addition to particle manipulation, electric fields can control fluid flow in microchannels. Arango et al. introduced a programmable microfluidic system with electroactuated valves to regulate liquid circuits⁶⁹ (Figure 7B).

Maintaining detecting performance over time requires consideration of the following factors: (1) medium conductivity and Joule heating: for example, when using culture medium (conductivity: 10– $100~\text{mS}\cdot\text{m}^{-1}$), applying several hundred volts can increase local fluid temperature by 10°C – 30°C within minutes. In contrast, switching to a low-conductivity medium ($\sim 1~\text{mS}\cdot\text{m}^{-1}$) limits the rise to 2°C – 4°C during 300~s operation. (2) Biosample sensitivity: for mammalian cells, $2~\text{kV}~\text{cm}^{-1}$ serves as an upper limit to avoid electroporation and viability loss (equivalent to 20~V for a 100- μm gap). This threshold should guide electrode spacing and drive choices. (3) Electrode stability under prolonged use: high electric fields in conductive buffers promote electrolysis, bubble formation, and electrode deterioration, which degrade DEP traps and flow uniformity. Countermeasures





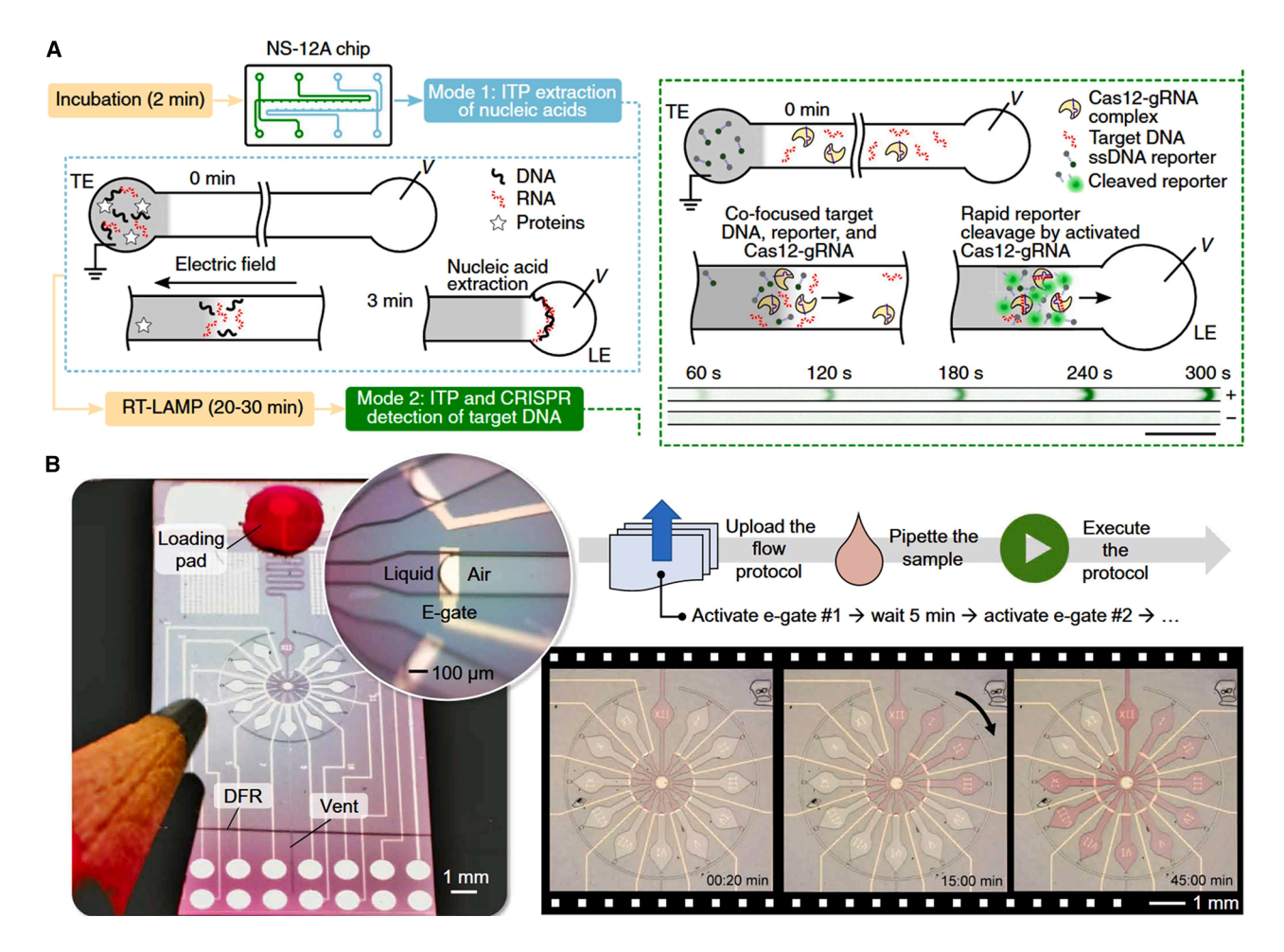


Figure 7. Microfluidic systems with manipulation electrodes to induce electric field

(A) Schematics of an electric-field-driven microfluidic chip operating in two modes: mode 1 enables isotachophoresis extraction for nucleic acid concentration and purification from impurities, while mode 2 employs CRISPR detection, with positive samples showing strong fluorescent signals compared to negative controls (copyright 2020, Proceedings of the National Academy of Sciences). 68

(B) A programmable microfluidic system controlling liquid circuits via electroactuated valves (e-gates) to form a "microfluidic clock." The chip after pipetting 3 µL of PBS with red dye: liquid travels through a 100-µm-wide, 15-mm-long channel and fills the clock's center within 20 s. Microscope images show e-gates automatically activated by a smartphone at 5-min intervals, marking the minutes of a 1-h clock (copyright 2020, American Association for the Advancement of Science). ⁶⁹

include operating at higher AC frequencies, using insulation layers, and periodically regenerating noble-metal electrodes electrochemically to restore surface activity. 72

Thermal field

When circuits are connected to electrodes, thermal fields arise, based on Joule's law, which can produce uniform or non-isothermal fields. Uniform-temperature fields, achieved through electrode heating, are typically used in applications such as polymerase chain reaction (PCR) and cell lysis. Due to their small scale, microfluidic systems can establish strong temperature gradients, creating non-isothermal fields that enable particle manipulation. Various physical mechanisms induced by these gradients facilitate controlling targets, including thermophoresis, thermocapillary, and thermal convection. ^{73,74}

Cong et al. developed a microfluidic system integrated with electrodes to trap target objects, e.g., PS spheres and live

cells, via thermophoresis.⁷⁵ Thermophoresis involves the direct migration of particles in a temperature gradient. As this gradient forms, buoyance forces drive thermal convection. Shen et al. combined thermophoresis and convection in a microfluidic system to control biological samples (Figure 8A).⁷⁶ Thermal convection can also be used to manipulate droplets, not just solid particles and cells. Zhang et al. designed a microfluidic platform with spiral electrodes for droplet migration, leveraging thermal convection (Figures 8B).⁷⁷ Because droplets exist in two-phase fluid systems (e.g., oil and water), temperature gradients at the interface can produce thermocapillary effects, which can be used to release particles from droplets.

Unlike electric field manipulation, temperature-based approaches place no restrictions on the solution's properties; however, because electrodes must locally generate high temperatures, this increases the design and placement requirements of the electrodes. The thermal effect of resistance



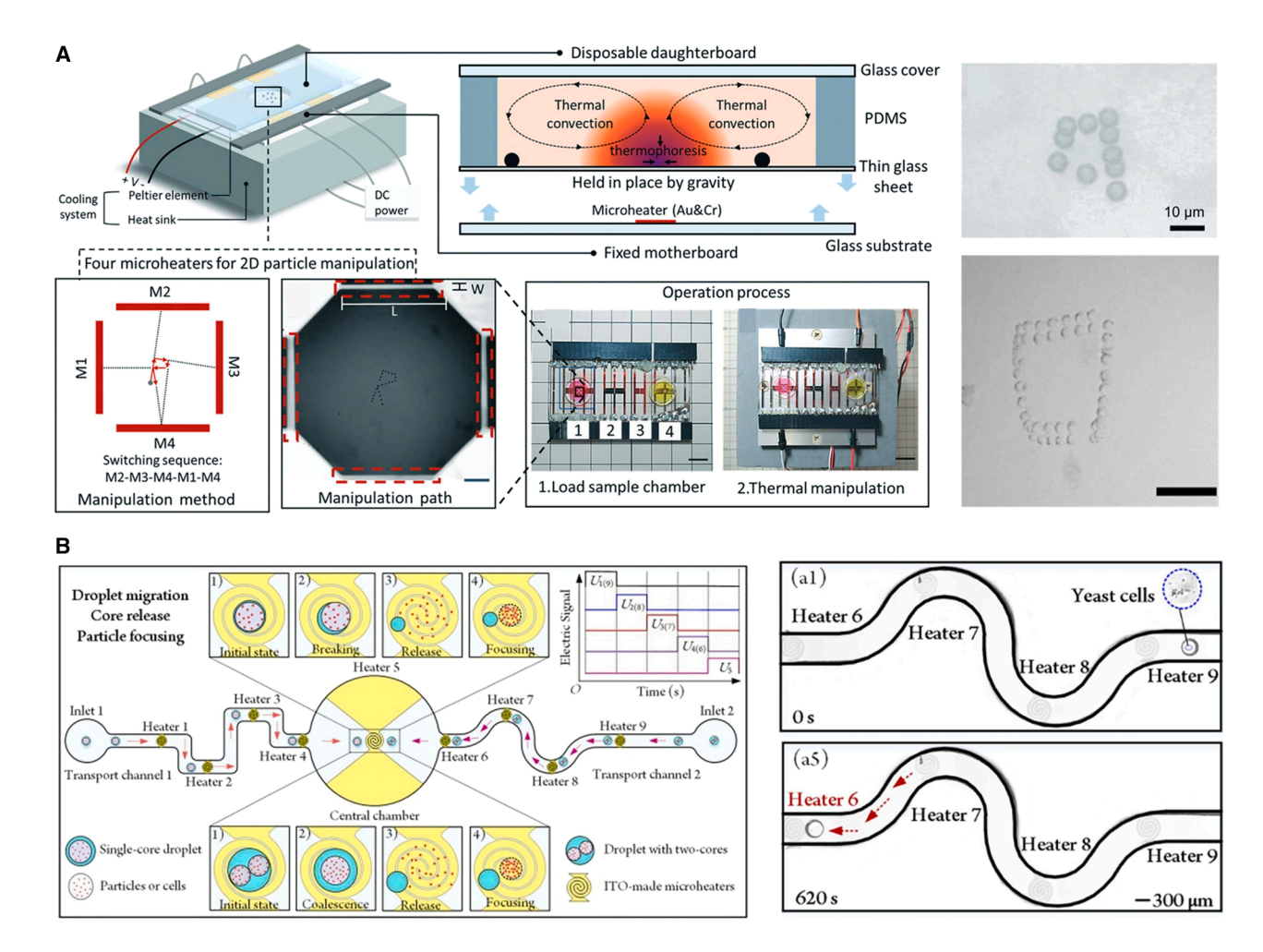


Figure 8. Microfluidic systems with manipulation electrodes to generate thermal fields

(A) An integrated microfluidic system with electrodes controlling sample movement via thermal convection. The system combines a disposable daughterboard (glass cover, PDMS channel, and thin glass sheet) with a fixed motherboard (glass patterned with Au and Cr electrodes). Four electrodes act as microheaters to manipulate particles (up) and cells (down) along distinct paths. Scalar bar, 150 µm (copyright 2020, The Royal Society of Chemistry).

(B) Schematics of a microfluidic platform with spiral electrodes for droplet migration via thermal convection. Multiple microheater electrodes positioned in the microchannel continuously manipulate droplets containing yeast cells (copyright 2022, Elsevier). 77

dictates that electrical energy converts to heat most efficiently at locations with the highest resistance. When designing heating electrodes, specific positions must be reserved within the manipulation area to form effective thermal fields. Standard heating electrode designs such as spiral, maze, serpentine, and ring patterns should be explored and optimized. These designs typically use planar configurations. More efficient heating control can be achieved by combining metal layers with different conductivities using MEMS technology, resulting in smaller and more efficient heating electrodes. Furthermore, multi-layer electrode arrangements enable the implementation of microheating electrode arrays.

Magnetic field

When spiral-shaped electrodes are used in a microfluidic system and an alternating electric field is applied, a magnetic field is formed. Lin et al. developed an automated microfluidic platform equipped with coil electrodes for nucleic acid detection suitable for simultaneous detection of various viruses (Figure 9A).⁸¹ By employing programmable coil electrodes, droplet manipulation was improved, enabling automatic control of the system.

As a non-contact method, these electrodes reduce considerable flexibility across various applications. However, the main limitation of magnetic field manipulation methods is their dependence on magnetic materials, especially when manipulating biological cells. Most cells and nucleic acids possess only weak diamagnetic properties; therefore, positive magnetophoresis typically requires labeling with superparamagnetic beads. Alia increases procedural steps and detection costs and introduces risks of non-specific binding. Label-free negative magnetophoresis avoids labeling issues but requires paramagnetic media (such as ferrofluids), which may alter sample viscosity and osmolarity, raising biocompatibility concerns. When using labels, the cytotoxicity and immune effects of





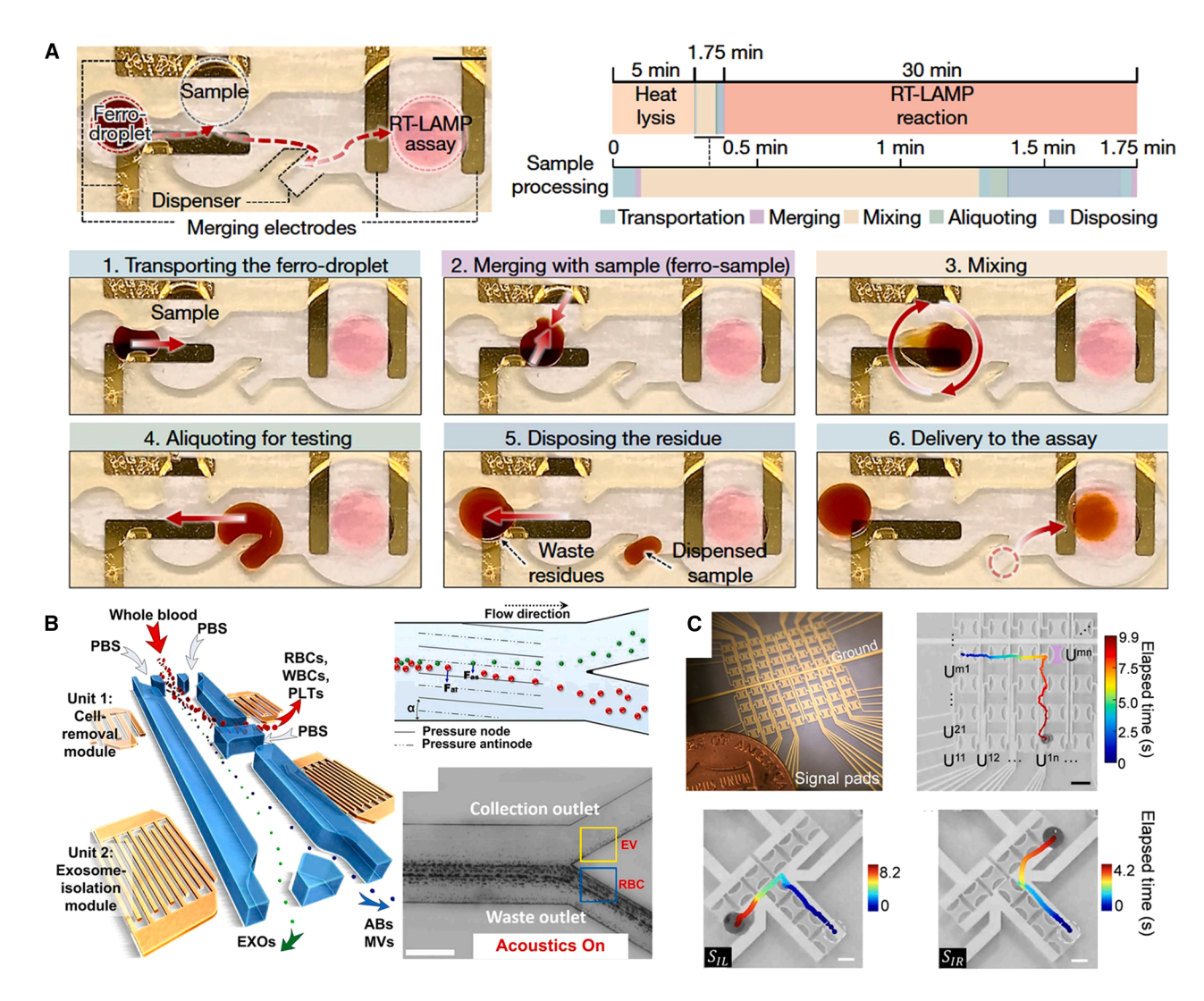


Figure 9. Microfluidic systems with manipulation electrodes to generate magnetic and acoustic fields

(A) Nucleic acid amplification testing on an automated system with coil electrodes for droplet manipulation: transporting, merging, mixing, aliquoting, disposing, and delivery (scale bar, 5 mm) (copyright 2022, Springer Nature).⁸¹

(B) An acoustic microfluidic system generating SSAWs for isolating blood cells and exosomes. SSAWs apply acoustic forces on target particles, enabling separation through designated exits. Scale bar, 500 µm (copyright 2017, Proceedings of the National Academy of Sciences). 82

(C) An array of 64 independent dual-mode interdigital transducers generating acoustic fields for droplet manipulation. Droplet movement along the transducer array. When droplets are held at U⁴⁴, the signal switches from the *x* axis to the *y* axis. Automated droplet routing (SIL, left turns; SIR, right turns). Scale bar, 500 μm (copyright 2020, American Association for the Advancement of Science).

superparamagnetic iron oxide nanoparticles are related to dosage and surface chemistry properties, highlighting the necessity of optimizing nanoparticle coating, charge, and washing steps. Electromagnetic coils, while providing reconfigurable magnetic fields, generate ohmic heating and power/packaging limitations. Even millimeter-scale printed circuit board (PCB) coils require thermal modeling and heat dissipation design, making sensor placement and temperature control particularly important in long-term detection.⁸⁶

Mechanical forces

When electrodes are fabricated on a piezoelectric substrate, mechanical vibrations occur via the piezoelectric effect, affecting

the movement of liquids and particles in microchannels. Cheng et al. introduced a microfluidic fluorescence-activated cell sorting (µFACS) microchip with integrated piezoelectric actuators for analysis and enrichment of mammalian cells. ⁸⁷ This disposable device provides a platform for fluorescence-based cell detection, helping to prevent cross-contamination and mitigate aerosol hazards. Microfluidic systems with piezoelectric actuators can be applied to cell sorting and droplet generation. Zhang and Xia used piezoelectric actuators to produce droplets with controllable volume and spacing. ⁸⁸

High-frequency mechanical vibrations can generate acoustic waves that control objects. Objects in a liquid can be manipulated through acoustic streaming, wherein acoustic waves





interact with fluid motion. Wu et al. fabricated a microfluidic system with crossed electrodes to generate standing surface acoustic waves (SSAWs) for exosome isolation from whole blood (Figure 9B).82 Its high efficiency and throughput make it promising for clinical exosome isolation and analysis. The same group also developed an electrode array to produce acoustic fields for droplet manipulation (Figure 9C).89 Despite its label-free and non-contact advantages, acoustic wave technology faces several challenges. Acoustothermal heating, directly linked to energy density and medium properties (e.g., conductivity and viscosity), can raise local temperatures enough to compromise cell viability and alter fluid characteristics. Additionally, ultrasound can generate fluid cavitation phenomena that disrupt experimental outcomes. 90 The competition between radiation force acoustophoresis and streaming-induced drag is sensitive to particle size, frequency, and fluid viscoelasticity. Even at moderate intensities, prolonged exposure to acoustic waves can damage cells through thermal effects or microstreaming shear, making biocompatibility assessment essential. To address these challenges, future research directions include: (1) developing phase-programmable, high-density phased arrays and harmonic field technologies to achieve real-time guidance of pressure nodes, supporting multiplexed analysis and adaptive sorting; (2) utilizing thin-film PZTs and MEMS to achieve low-power, flexible, and monolithically integrated acoustic systems; and (3) optimizing the balance between acoustic energy density and thermal management. 92 Next-generation acoustic devices with mechanics-coupled designs can enhance acoustic force transmission efficiency while controlling heat load, meeting the requirements for clinical-scale processing.

CONCLUSION AND OUTLOOK

Microfluidic technology enables the handling, storage, and analysis of biological samples in spatially defined regions. Electrodes play a critical role in these systems by endowing microfluidic chips with the abilities to detect and manipulate samples. These devices need to focus on improving precision, expanding comprehensive capabilities, and enhancing intelligence. To address these objectives, we propose the following avenues for future investigation.

Electrode fabrication

Photolithography remains the preferred method for electrode fabrication owing to its high precision and alignment accuracy; however, when applied to microfluidic devices with integrated electrodes, it faces several limitations. First, many electrode functions require thick or 3D structures such as pillars, sidewall contact points, and embedded contact pads. Fabricating such 3D structures poses challenges for photolithography, as it typically needs multiple processes of patterning and alignment, leading to complex and time-consuming workflows. Yadav et al. developed a template-assisted electroplating method that uses an ultrasonic process to maintain uniform deposition in 3D microelectrode arrays. 93 Second, metal adhesion layer durability presents a challenge for electrodes in aqueous environments. Au on Cr, for example, can undergo undercutting when exposed to AC fields, resulting in edge liftoff and delamina-

tion.94 Third, creating stable metal patterns directly on elastomers remains problematic due to the poor adhesion between Au and PDMS. Furthermore, once electrodes are fabricated on solid substrates, their static structure cannot be reconfigured or adjusted after manufacturing.

Next-generation electrode processing technology needs to expand in the following areas: (1) more efficient 3D electrode manufacturing methods such as light-based additive manufacturing, including SLA and multi-photon lithography (MPL). SLA uses UV lasers to construct macroscopic 3D structures by sequentially curing photosensitive resins (achieving resolution of approximately 10 μm), while MPL leverages focused multi-photon absorption to achieve nanometer precision. SLA offers advantages for prototype and mold fabrication with faster printing speeds and lower costs, while MPL specializes in micro/nano manufacturing with exceptional resolution. Brown et al. used MPL technology to develop a process for fabricating 3D electrodes with micrometer-level resolution on flexible substrates (maximum height of 3D structures limited to a few micrometers), which can effectively record electrical signals from neural activity in small animals.95 (2) Electrode stability enhancement such as by replacing Cr with alternative adhesion layer strategies, electroplating Au to prevent corrosion, adding thin parylene or atomic layer deposition passivation layers, or embedding metals into elastomers to create contact points that resist stretching and washing.⁹⁶ (3) Three-dimensional flexible electrodes: while planar electrodes benefit from the MEMS miniaturization for microfluidic channels, their rigidity can lead to tissue damage and inflammation during long-term implantation.91 Three-dimensional flexible electrodes employ stretchable nonplanar structures that conform precisely to biological tissues or organoids, significantly enhancing long-term stability, spatial resolution, and signal quality in biological detection. Park et al. used 3D flexible mesh electrodes for real-time monitoring of brain organoids. 98 Three-dimensional flexible electrodes feature innovative designs such as ultrathin metal serpentine traces embedded in elastomers, mesh structures that envelop spheroids, and microstructures that soften after insertion.95

Multi-functional electrode integration

Electrode-enabled microfluidic chips often perform detection and actuation separately, though some integrated electrode microfluidic systems already exist for cell sorting applications. The integration of different electrodes presents challenges due to their operational requirements. Sensing electrodes (used in electrochemical detection like impedance analysis and amperometry) require low noise and small excitation signals to minimize electrode polarization. In contrast, manipulation electrodes (for DEP, thermophoresis, and ultrasonics) typically need higher voltage and frequency drives. In electrode integration systems, these manipulation electrodes introduce electromagnetic interference and heat into nearby sensing electrodes. Several strategies can reduce these interactions, including frequencydivision or time-division separation of sensing and actuation, physical isolation and shielding between electrode types, and remote placement of REs for electrochemical readouts. 100

Brain-on-chip (BoC) platforms create micro physiological models of neural tissue and neurovascular units on microfluidic





chips. BoC platforms need to simultaneously handle fluid actuation, cell stimulation, and drug release, requiring complex microchannel and electrode structures for high-precision measurement and control. ^{98,101} Future research in multi-functional electrode integration will focus on two key directions: (1) "release + detection" microfluidic electrode chips; for example, PEDOT-based microelectrodes electrically release glutamate/ GABA while nearby microsensors quantify nitric oxide or neurotransmitter responses within seconds, enabling closed-loop perturbation and measurement experiments. ¹⁰² (2) "Detection + screening" microfluidic chips, for example, DEP enrichment with online impedance cell counting, where sorting on one frequency band is monitored by label-free impedance metrics on another band, providing feedback while limiting interference. ¹⁰³

Solid-liquid interface interactions of electrodes

Microfluidic electrodes can use liquid substrates instead of rigid metals to reduce interface impedance, improve contact, and allow reconfiguration after fabrication. (1) Liquid metals (such as EGaln/Galinstan) can replace solid metal electrodes by filling microchannels. Their bulk-like conductivity and flow properties enable self-healing, reshaping, and rewiring capabilities. However, their packaging design must prevent liquid metal from causing embrittlement of certain metals and ensure biocompatibility in exposed areas. 104 (2) Conductive hydrogels (such as PEDOT/PSS or nanocarbon enhanced) provide tissuelike, water-rich interfaces that can replace traditional electrode surfaces. These hydrogels maintain low impedance while reducing micromotion damage, which is an important feature for signal detection in organ-on-chip and brain-on-chip devices. 105 (3) Ionic liquid (IL) junctions and gel salt bridges can replace conventional RE junctions, effectively preventing evaporation and junction potential drift in small-volume systems. 106 (4) Slippery liquid-infused porous surfaces (SLIPS) can serve as dielectric/passivation layers on electrodes, inhibiting biofouling and preventing bubble adhesion. 107 This stabilizes long-term electrochemical performance in protein-rich media.

Integrated electrode microfluidic chips are developing toward portable sensing units and high-precision detection systems, in particular for POCT applications. Scalable solid-state ISEs can be embedded in microchannels carrying sweat or urine to enable online electrolyte monitoring, 108 amplification-free peptide nucleic acid (PNA) detection units can be integrated into disposable cartridge chips for screening low-copy pathogenic nucleic acids, 83 and molecularly imprinted lossy mode resonance (LMR) optical sensors can be integrated with on-chip waveguides or optical windows for selective detection of molecule biomarkers. 109 These technologies combine enhanced material-level specificity with precise chip-level fluid control, addressing needs such as parallel multi-indicator detection, minimal sample consumption, pump-free operation, and mobile readout capabilities.

The development of artificial intelligence (Al) technology and large predictive models creates opportunities for designing and fabricating next-generation electrodes. 110,111 Beyond accelerating the R&D cycle, Al enables data-driven calibration of multiplexed signals and closed-loop thermal control. In data-driven calibration of multiplexed electrical signals, machine

learning models can separate and correct crosstalk and drift in multi-electrode readings. This improves identification and quantification capabilities without requiring single-device calibration. For closed-loop temperature control, Al controllers and visual feedback can reduce the trial-and-error iterations needed for PCR/heater arrays to achieve and maintain target temperatures. Combining on-chip sensors with learning-based calibration and control is crucial for next-generation microfluidic chips featuring high-density electrode arrays.

In sensing electrode design, such as electrochemical measurement, the electrode geometry and layout determine detection sensitivity. Classical optimization models (such as genetic algorithms and topology optimization) have been extended to Bayesian optimization or deep surrogate models, which learn objective functions through simulation and experimental data, reducing the simulation burden and improving performance. 112,113 In impedance cytometry, specific electrode shapes (such as coplanar electrodes and bypass/ground electrodes) have been shown to improve sensitivity and expand the range of detectable particle sizes. 114,115 Integrating these parameters with AI can enhance signal accuracy and reliability. AI can be used for the simulation of physical fields such as electric and thermal fields for optimizing the fabrication of electrodes with improved spatial controllability. In droplet microfluidic chips with electrode arrays, researchers have used deep reinforcement learning and semantic segmentation vision models to create defect-resistant droplet paths, manage parallel scheduling, and recognize system states. These technologies can perform mixing, distribution, and parallel reaction sequences without human oversight. 116,117 Microheater electrodes are used in PCR, lysis, mixing, and thermocapillary control; however, spatial temperature non-uniformity can reduce their performance. Recurrent neural networks (RNNs) have been used to reconstruct the on-chip temperature distribution from fluorescence signals, achieving a root-mean-square error of sub-0.1 K compared to a validated COMSOL model, demonstrating that learning agents can infer the complete thermal field from sparse or indirect measurements. 118 Meanwhile, physics-informed neural network (PINN) frameworks for heat transfer and electrokinetic microfluidics provide data-efficient, reliable solvers that can be embedded in model predictive control (MPC) or reinforcement learning systems to maintain precise temperature distributions even when load conditions change. 119 These methods enable verification of heater performance during the design phase and enable the prediction of microheater thermal field distribution using machine learning. Unlike laser-focused heat sources, electrodes face size limitations that restrict their ability to create smaller thermal points. Laser heating based on photothermal effects provides advantages through light spot focusing and positional flexibility. Schmidt et al. demonstrated this by using gold nanorods to generate reconfigurable microscale thermal barriers within microchannels, enabling real-time particle sorting. 120 This approach remains underexplored in electrode microheater development. Combining Al design with precision MEMS technology to create reconfigurable thermal barriers for microelectrodes represents a promising future research direction.

We have discussed various aspects of electrodes in microfluidic systems, covering fundamental fabrication methods,





the latest advancements in biochemistry, and current opportunities and challenges. By categorizing electrodes into sensing and manipulation types, researchers from diverse fields can more easily understand the technology and adapt it to their work. Developments in these emerging microfluidic electrode systems are poised to drive transformative applications in biomedicine, environmental monitoring, and chemical analysis.

ACKNOWLEDGMENTS

This work was supported by the National Natural Science Foundation of China (22304143, 22275156, 52025132, and U24A20205), the Zhejiang Provincial Natural Science Foundation of China (LQN25E050020, LZ24E050008, and LY24E050006), the Open Fund Project of the Key Laboratory of CNC Equipment Reliability, Ministry of Education (JLU-cncr-202407), The Key Science and Technology Plan Project of Jinhua City, China (2023-3-084), and the New Cornerstone Science Foundation through the XPLORER PRIZE.

AUTHOR CONTRIBUTIONS

Y.S. and H.L. designed the review framework, conducted the literature review, and wrote the paper, which was revised by Jin Li, X.H., and J.W. H.L., Y.L., Y.W., K.C., Jianping Li, J.M., Y.H., and K.C. provided support, contributed to writing, and participated in discussions for the review.

DECLARATION OF INTERESTS

The authors declare no competing interests.

SUPPLEMENTAL INFORMATION

Supplemental information can be found online at https://doi.org/10.1016/j.device.2025.100964.

REFERENCES

- Sharma, B., and Sharma, A. (2022). Microfluidics: Recent Advances Toward Lab-on-Chip Applications in Bioanalysis. Adv. Eng. Mater. 24, 2100738. https://doi.org/10.1002/adem.202100738.
- Ingber, D.E. (2022). Human organs-on-chips for disease modelling, drug development and personalized medicine. Nat. Rev. Genet. 23, 467–491. https://doi.org/10.1038/s41576-022-00466-9.
- Adekanmbi, E.O., and Srivastava, S.K. (2019). Dielectric characterization of bioparticles via electrokinetics: The past, present, and the future. Appl. Phys. Rev. 6, 041313. https://doi.org/10.1063/1.5113709.
- Birch, C., and Landers, J. (2017). Electrode Materials in Microfluidic Systems for the Processing and Separation of DNA: A Mini Review. Micromachines 8, 76. https://doi.org/10.3390/mi8030076.
- Ju, F., Wang, Y., Yin, B., Zhao, M., Zhang, Y., Gong, Y., and Jiao, C. (2023). Microfluidic Wearable Devices for Sports Applications. Micromachines 14, 1792. https://doi.org/10.3390/mi14091792.
- Jang, J., Song, Y., Yoo, D., Ober, C.K., Lee, J.-K., and Lee, T. (2016). The development of fluorous photolithographic materials and their applications to achieve flexible organic electronic devices. Flex. Print. Electron. 1, 023001. https://doi.org/10.1088/2058-8585/1/2/023001.
- Lee, J.N., Park, C., and Whitesides, G.M. (2003). Solvent Compatibility of Poly(dimethylsiloxane)-Based Microfluidic Devices. Anal. Chem. 75, 6544–6554. https://doi.org/10.1021/ac0346712.
- Giboz, J., Copponnex, T., and Mélé, P. (2007). Microinjection molding of thermoplastic polymers: a review. J. Micromech. Microeng. 17, R96–R109. https://doi.org/10.1088/0960-1317/17/6/R02.

- Wu, J., and Gu, M. (2011). Microfluidic sensing: state of the art fabrication and detection techniques. J. Biomed. Opt. 16, 080901. https://doi.org/ 10.1117/1.3607430.
- 10. Gilleo, K., Murray, J., and Fab, P. 1999 The Definitive History of the Printed Circuit.
- Wiklund, J., Karakoç, A., Palko, T., Yiğitler, H., Ruttik, K., Jäntti, R., and Paltakari, J. (2021). A Review on Printed Electronics: Fabrication Methods, Inks, Substrates, Applications and Environmental Impacts. J. Manuf. Mater. Process. 5, 89. https://doi.org/10.3390/jmmp5030089.
- Campos-Arias, L., Peřinka, N., Lau, Y.C., Castro, N., Pereira, N., Correia, V.M.G., Costa, P., Vilas-Vilela, J.L., and Lanceros-Mendez, S. (2024). Improving Definition of Screen-Printed Functional Materials for Sensing Application. ACS Appl. Electron. Mater. 6, 2152–2160. https://doi.org/ 10.1021/acsaelm.3c01415.
- Rama, E.C., and Costa-García, A. (2016). Screen-printed Electrochemical Immunosensors for the Detection of Cancer and Cardiovascular Biomarkers. Electroanalysis 28, 1700–1715. https://doi.org/10.1002/elan.201600126.
- Ahmed, M.U., Hossain, M.M., Safavieh, M., Wong, Y.L., Abd Rahman, I., Zourob, M., and Tamiya, E. (2016). Toward the development of smart and low cost point-of-care biosensors based on screen printed electrodes. Crit. Rev. Biotechnol. 36, 495–505. https://doi.org/10.3109/07388551. 2014.992387.
- Kukkola, J., Mohl, M., Leino, A.-R., Tóth, G., Wu, M.-C., Shchukarev, A., Popov, A., Mikkola, J.-P., Lauri, J., Riihimäki, M., et al. (2012). Inkjetprinted gas sensors: metal decorated WO3 nanoparticles and their gas sensing properties. J. Mater. Chem. 22, 17878–17886. https://doi.org/ 10.1039/C2JM32499G.
- Beedasy, V., and Smith, P.J. (2020). Printed Electronics as Prepared by Inkjet Printing. Materials 13, 704. https://doi.org/10.3390/ma13030704.
- Bernasconi, R., Brovelli, S., Viviani, P., Soldo, M., Giusti, D., and Magagnin, L. (2022). Piezoelectric Drop-On-Demand Inkjet Printing of High-Viscosity Inks. Adv. Eng. Mater. 24, 2100733. https://doi.org/10. 1002/adem.202100733.
- Kamarudin, S.F., Abdul Aziz, N.H., Lee, H.W., Jaafar, M., and Sulaiman, S. (2024). Inkjet Printing Optimization: Toward Realization of High-Resolution Printed Electronics. Adv. Mater. Technol. 9, 2301875. https://doi.org/10.1002/admt.202301875.
- Sliz, R., Czajkowski, J., and Fabritius, T. (2020). Taming the Coffee Ring Effect: Enhanced Thermal Control as a Method for Thin-Film Nanopatterning. Langmuir 36, 9562–9570. https://doi.org/10.1021/acs.langmuir.0c01560.
- Zhang, M., Chen, J., Zhu, J., Tao, Z., and Qiu, L. (2024). Hybrid manipulation of inkjet-printing deposition pattern of high particle concentration droplet by means of thermal and binary solvent effects. Int. J. Heat Mass Tran. 223, 125225. https://doi.org/10.1016/j.ijheatmasstransfer. 2024.125225.
- Balliu, E., Andersson, H., Engholm, M., Öhlund, T., Nilsson, H.-E., and Olin, H. (2018). Selective laser sintering of inkjet-printed silver nanoparticle inks on paper substrates to achieve highly conductive patterns. Sci. Rep. 8, 10408. https://doi.org/10.1038/s41598-018-28684-4.
- Majee, S., Karlsson, M.C.F., Wojcik, P.J., Sawatdee, A., Mulla, M.Y., Alvi, N.u.H., Dyreklev, P., Beni, V., and Nilsson, D. (2021). Low temperature chemical sintering of inkjet-printed Zn nanoparticles for highly conductive flexible electronic components. npj Flex. Electron. 5, 14. https:// doi.org/10.1038/s41528-021-00111-1.
- Embia, G., Moharana, B.R., Mohamed, A., Muduli, K., and Muhammad, N.B. (2023). 3D Printing Pathways for Sustainable Manufacturing. In New Horizons for Industry 4.0 in Modern Business, A. Nayyar, M. Naved, and R. Rameshwar, eds. (Springer International Publishing), pp. 253–272. https://doi.org/10.1007/978-3-031-20443-2_12.

DeviceReview



- Kalkal, A., Kumar, S., Kumar, P., Pradhan, R., Willander, M., Packirisamy, G., Kumar, S., and Malhotra, B.D. (2021). Recent advances in 3D printing technologies for wearable (bio)sensors. Addit. Manuf. 46, 102088. https://doi.org/10.1016/j.addma.2021.102088.
- Deka, M., Sinha, N., Das, R., Hazarika, N.K., Das, H., Daurai, B., and Gogoi, M. (2024). A review on the surface modification of materials for 3D-printed diagnostic devices. Anal. Methods 16, 485–495. https://doi. org/10.1039/D3AY01742G.
- Scheideler, W.J., and Im, J. (2025). Recent Advances in 3D Printed Electrodes Bridging the Nano to Mesoscale. Adv. Sci. 12, 2411951. https://doi.org/10.1002/advs.202411951.
- Arias-Ferreiro, G., Ares-Pernas, A., Dopico-García, M.S., Lasagabáster-Latorre, A., and Abad, M.-J. (2020). Photocured conductive PANI/acrylate composites for digital light processing. Influence of HDODA crosslinker in rheological and physicochemical properties. Eur. Polym. J. 136, 109887. https://doi.org/10.1016/j.eurpolymj.2020.109887.
- Ursi, F., and De Pasquale, G. (2025). Comparative characterization of FDM structures with electrically-conductive sensing elements under static, dynamic and thermal loads. Sci. Rep. 15, 26877. https://doi.org/ 10.1038/s41598-025-11234-0.
- Tian, H., Guo, H., Zhang, H., Zhang, T., Tang, Y., Ye, Z., Zhang, J., Yuan, G., Zhou, Q., Li, Y., et al. (2025). Toxicity of stereolithography 3D printed objects at the chemical level and strategies to improve biocompatibility. Addit. Manuf. 101, 104715. https://doi.org/10.1016/ j.addma.2025.104715.
- Bartholomeusz, D.A., Boutte, R.W., and Andrade, J.D. (2005). Xurography: rapid prototyping of microstructures using a cutting plotter.
 J. Microelectromech. Syst. 14, 1364–1374. https://doi.org/10.1109/JMFMS.2005.859087
- Kongkaew, S., Meng, L., Limbut, W., Liu, G., Kanatharana, P., Thavarungkul, P., and Mak, W.C. (2023). Craft-and-Stick Xurographic Manufacturing of Integrated Microfluidic Electrochemical Sensing Platform. Biosensors 13, 446. https://doi.org/10.3390/bios13040446.
- Wu, M., Gao, Y., Ghaznavi, A., Zhao, W., and Xu, J. (2022). AC electroosmosis micromixing on a lab-on-a-foil electric microfluidic device. Sensor. Actuator. B Chem. 359, 131611. https://doi.org/10.1016/j.snb.2022. 131611.
- Cai, X., Xia, R.-Z., Liu, Z.-H., Dai, H.-H., Zhao, Y.-H., Chen, S.-H., Yang, M., Li, P.-H., and Huang, X.-J. (2024). Fully Integrated Multiplexed Wristwatch for Real-Time Monitoring of Electrolyte Ions in Sweat. ACS Nano 18, 12808–12819. https://doi.org/10.1021/acsnano.3c13035.
- 34. Pagkali, V., Soulis, D., Kokkinos, C., and Economou, A. (2022). Fully drawn electrochemical paper-based glucose biosensors fabricated by a high-throughput dual-step pen-on-paper approach with commercial writing stationery. Sensor. Actuator. B Chem. 358, 131546. https://doi.org/10.1016/j.snb.2022.131546.
- Jeong, S.H., Hjort, K., and Wu, Z. (2014). Tape Transfer Printing of a Liquid Metal Alloy for Stretchable RF Electronics. Sensors 14, 16311– 16321. https://doi.org/10.3390/s140916311.
- Seker, E., Reed, M.L., and Begley, M.R. (2009). Nanoporous Gold: Fabrication, Characterization, and Applications. Materials 2, 2188–2215. https://doi.org/10.3390/ma2042188.
- Douville, N.J., Tung, Y.-C., Li, R., Wang, J.D., El-Sayed, M.E.H., and Takayama, S. (2010). Fabrication of Two-Layered Channel System with Embedded Electrodes to Measure Resistance Across Epithelial and Endothelial Barriers. Anal. Chem. 82, 2505–2511. https://doi.org/10. 1021/ac9029345.
- Tsao, C.-W., and DeVoe, D.L. (2009). Bonding of thermoplastic polymer microfluidics. Microfluid Nanofluid 6, 1–16. https://doi.org/10.1007/ s10404-008-0361-x.
- 39. Li, S.-C., Chiang, C.-C., Tsai, Y.-S., Chen, C.-J., and Lee, T.-H. (2024). Fabrication of a Three-Dimensional Microfluidic System from Poly(methyl

- methacrylate) (PMMA) Using an Intermiscibility Vacuum Bonding Technique. Micromachines 15, 454. https://doi.org/10.3390/mi15040454.
- Gou, P., Meng, S., Yan, H., Liu, J., Chen, N., and Zhao, Y. (2024). Machining technologies and structural models of microfluidic devices. Proc. IME C J. Mech. Eng. Sci. 238, 8294–8329. https://doi.org/10. 1177/09544062241237705.
- Le Berre, M., Crozatier, C., Velve Casquillas, G., and Chen, Y. (2006). Reversible assembling of microfluidic devices by aspiration. Microelectron. Eng. 83, 1284–1287. https://doi.org/10.1016/j.mee.2006.01.257.
- Wang, J. (2006). Electrochemical biosensors: Towards point-of-care cancer diagnostics. Biosens. Bioelectron. 21, 1887–1892. https://doi. org/10.1016/j.bios.2005.10.027.
- Pumera, M., Merkoçi, A., and Alegret, S. (2006). New materials for electrochemical sensing VII. Microfluidic chip platforms. TrAC, Trends Anal. Chem. 25, 219–235. https://doi.org/10.1016/j.trac.2005.08.005.
- 44. Ma, S., Zhao, W., Liu, X., Li, Y., Ma, P., Zhang, K., and Zhang, Q. (2024). A novel microfluidic chip integrating with microcolumn array electrodes for rapid and ultrasensitive detection of alpha-fetoprotein. Anal. Chim. Acta 1291, 342240. https://doi.org/10.1016/j.aca.2024.342240.
- 45. Fu, H., Qin, Z., Li, X., Pan, Y., Xu, H., Pan, P., Song, P., and Liu, X. (2023). Paper-Based All-in-One Origami Nanobiosensor for Point-of-Care Detection of Cardiac Protein Markers in Whole Blood. ACS Sens. 8, 3574–3584. https://doi.org/10.1021/acssensors.3c01221.
- Zhong, B., Qin, X., Xu, H., Liu, L., Li, L., Li, Z., Cao, L., Lou, Z., Jackman, J.A., Cho, N.-J., and Wang, L. (2024). Interindividual- and bloodcorrelated sweat phenylalanine multimodal analytical biochips for tracking exercise metabolism. Nat. Commun. 15, 624. https://doi.org/ 10.1038/s41467-024-44751-z.
- Shi, Z., Deng, P., Zhou, L., Jin, M., Fang, F., Chen, T., Liu, G., Wen, H., An, Z., Liang, H., et al. (2024). Wireless and battery-free wearable biosensing of riboflavin in sweat for precision nutrition. Biosens. Bioelectron. 251, 116136. https://doi.org/10.1016/j.bios.2024.116136.
- Phoonsawat, K., Ozer, T., Dungchai, W., and Henry, C.S. (2022). Dual-mode ion-selective electrodes and distance-based microfluidic device for detection of multiple urinary electrolytes. Analyst 147, 4517–4524. https://doi.org/10.1039/D2AN01220K.
- Zhang, Z., Boselli, E., and Papautsky, I. (2023). Potentiometric Sensor System with Self-Calibration for Long-Term, In Situ Measurements. Chemosensors 11, 48. https://doi.org/10.3390/chemosensors11010048.
- Wei, L., Lv, Z., He, Y., Cheng, L., Qiu, Y., Huang, X., Ding, C., Wu, H., and Liu, A. (2023). In-situ admittance sensing of sweat rate and chloride level in sweat using wearable skin-interfaced microfluidic patch. Sensor. Actuator. B Chem. 379, 133213. https://doi.org/10.1016/j.snb.2022.133213.
- Lim, H.-R., Lee, S.M., Park, S., Choi, C., Kim, H., Kim, J., Mahmood, M., Lee, Y., Kim, J.-H., and Yeo, W.-H. (2022). Smart bioelectronic pacifier for real-time continuous monitoring of salivary electrolytes. Biosens. Bioelectron. 210, 114329. https://doi.org/10.1016/j.bios.2022.114329.
- Zhang, W., Wang, S., Kang, D., Xiong, Z., Huang, Y., Ma, L., Liu, Y., Zhao, W., Chen, S., and Xu, Y. (2024). Integrated Microfluidic Chip Technology for Copper Ion Detection Using an All-Solid-State Ion-Selective Electrode. Micromachines 15, 160. https://doi.org/10.3390/mi15010160.
- Bahadır, E.B., and Sezgintürk, M.K. (2016). A review on impedimetric biosensors. Artif. Cells, Nanomed. Biotechnol. 44, 248–262. https://doi.org/10.3109/21691401.2014.942456.
- 54. Ben Messaoud, N., Barreiros dos Santos, M., Trocado, V., Nogueira-Silva, C., and Queirós, R. (2023). A novel label-free electrochemical immunosensor for detection of surfactant protein B in amniotic fluid. Talanta 251, 123744. https://doi.org/10.1016/j.talanta.2022.123744.
- Ehzari, H., Safari, M., Hallaj, R., and Amiri, M. (2024). Electrochemical microfluidic paper-based analytical device for label-free detection of SARS-CoV-2 antigen by LDH redox probe. Microchem. J. 197, 109779. https://doi.org/10.1016/j.microc.2023.109779.





- Schwarz, M., Jendrusch, M., and Constantinou, I. (2020). Spatially resolved electrical impedance methods for cell and particle characterization. Electrophoresis 41, 65–80. https://doi.org/10.1002/elps.201900286.
- Zhu, J., Pan, S., Chai, H., Zhao, P., Feng, Y., Cheng, Z., Zhang, S., and Wang, W. (2024). Microfluidic Impedance Cytometry Enabled One-Step Sample Preparation for Efficient Single-Cell Mass Spectrometry. Small 20, 2310700. https://doi.org/10.1002/smll.202310700.
- Tang, T., Liu, X., Kiya, R., Shen, Y., Yuan, Y., Zhang, T., Suzuki, K., Tanaka, Y., Li, M., Hosokawa, Y., and Yalikun, Y. (2021). Microscopic impedance cytometry for quantifying single cell shape. Biosens. Bioelectron. 193, 113521. https://doi.org/10.1016/j.bios.2021.113521.
- Güvener, N., Oguzhan Caglayan, M., and Altintas, Z. (2023). 8 Surface plasmon resonance sensors. In Fundamentals of Sensor Technology Woodhead Publishing Series in Electronic and Optical Materials, A. Barhoum and Z. Altintas, eds. (Woodhead Publishing), pp. 163–196. https:// doi.org/10.1016/B978-0-323-88431-0.00001-6.
- 60. Qu, J.-H., Ordutowski, H., Van Tricht, C., Verbruggen, R., Barcenas Gallardo, A., Bulcaen, M., Ciwinska, M., Gutierrez Cisneros, C., Devriese, C., Guluzade, S., et al. (2022). Point-of-care therapeutic drug monitoring of adalimumab by integrating a FO-SPR biosensor in a self-powered microfluidic cartridge. Biosens. Bioelectron. 206, 114125. https://doi.org/10.1016/j.bios.2022.114125.
- Lin, T., Huang, Y., Zhong, S., Shi, T., Sun, F., Zhong, Y., Zeng, Q., Zhang, Q., and Cui, D. (2024). Passive trapping of biomolecules in hotspots with all-dielectric terahertz metamaterials. Biosens. Bioelectron. 251, 116126. https://doi.org/10.1016/j.bios.2024.116126.
- Gubeljak, P., Xu, T., Pedrazzetti, L., Burton, O.J., Magagnin, L., Hofmann, S., Malliaras, G.G., and Lombardo, A. (2023). Electrochemically-gated graphene broadband microwave waveguides for ultrasensitive biosensing. Nanoscale 15, 15304–15317. https://doi.org/10.1039/D3NR01239E.
- Silver, K., Li, J., Porch, A., Jamieson, W.D., Castell, O., Dimitriou, P., Kallnik, C., and Barrow, D. (2024). 3D-printed microfluidic–microwave device for droplet network formation and characterisation. Lab Chip 24, 5101–5112. https://doi.org/10.1039/D4LC00387J.
- Huang, X., Wang, Y., Li, X., and Liu, T. (2024). Minimal microfluidic metamaterial sensor for concentration detection. Measurement 224, 113864. https://doi.org/10.1016/j.measurement.2023.113864.
- Li, J., Jamieson, W.D., Dimitriou, P., Xu, W., Rohde, P., Martinac, B., Baker, M., Drinkwater, B.W., Castell, O.K., and Barrow, D.A. (2022). Building programmable multicompartment artificial cells incorporating remotely activated protein channels using microfluidics and acoustic levitation. Nat. Commun. 13, 4125. https://doi.org/10.1038/s41467-022-31898-w.
- Li, J., Baxani, D.K., Jamieson, W.D., Xu, W., Rocha, V.G., Barrow, D.A., and Castell, O.K. (2020). Formation of Polarized, Functional Artificial Cells from Compartmentalized Droplet Networks and Nanomaterials, Using One-Step, Dual-Material 3D-Printed Microfluidics. Adv. Sci. 7, 1901719. https://doi.org/10.1002/advs.201901719.
- Çetin, B., and Li, D. (2011). Dielectrophoresis in microfluidics technology. Electrophoresis 32, 2410–2427. https://doi.org/10.1002/elps.201100167.
- Ramachandran, A., Huyke, D.A., Sharma, E., Sahoo, M.K., Huang, C., Banaei, N., Pinsky, B.A., and Santiago, J.G. (2020). Electric field-driven microfluidics for rapid CRISPR-based diagnostics and its application to detection of SARS-CoV-2. Proc. Natl. Acad. Sci. USA 117, 29518– 29525. https://doi.org/10.1073/pnas.2010254117.
- Arango, Y., Temiz, Y., Gökçe, O., and Delamarche, E. (2020). Electroactuated valves and self-vented channels enable programmable flow control and monitoring in capillary-driven microfluidics. Sci. Adv. 6, eaay8305. https://doi.org/10.1126/sciadv.aay8305.
- Salari, A., Navi, M., Lijnse, T., and Dalton, C. (2019). AC Electrothermal Effect in Microfluidics: A Review. Micromachines 10, 762. https://doi. org/10.3390/mi10110762.

- de Wijs, K., Liu, C., Dusa, A., Vercruysse, D., Majeed, B., Tezcan, D.S., Blaszkiewicz, K., Loo, J., Lagae, L., Liu, J., et al. (2014). Single cell viability observation in cell dielectrophoretic trapping on a microchip. Appl. Phys. Lett. 104, 013703. https://doi.org/10.1063/1.4861135.
- Lee, J., Suh, H.N., Park, H.B., Park, Y.M., Kim, H.J., and Kim, S. (2023). Regenerative Strategy of Gold Electrodes for Long-Term Reuse of Electrochemical Biosensors. ACS Omega 8, 1389–1400. https://doi.org/10.1021/acsomega.2c06851.
- Tian, F., Han, Z., Deng, J., Liu, C., and Sun, J. (2021). Thermomicrofluidics for biosensing applications. View 2, 20200148. https://doi.org/10.1002/VIW.20200148.
- Zhang, K., Ren, Y., Hou, L., Tao, Y., Liu, W., Jiang, T., and Jiang, H. (2019). Continuous microfluidic mixing and the highly controlled nanoparticle synthesis using direct current-induced thermal buoyancy convection. Microfluid Nanofluid 24, 1. https://doi.org/10.1007/s10404-019-2306-y.
- Cong, H., Chen, J., and Ho, H.-P. (2018). Trapping, sorting and transferring of micro-particles and live cells using electric current-induced thermal tweezers. Sensor. Actuator. B Chem. 264, 224–233. https:// doi.org/10.1016/j.snb.2018.02.016.
- Shen, Y., Yalikun, Y., Aishan, Y., Tanaka, N., Sato, A., and Tanaka, Y. (2020). Area cooling enables thermal positioning and manipulation of single cells. Lab Chip 20, 3733–3743. https://doi.org/10.1039/D0LC00523A.
- Zhang, K., Ren, Y., Jiang, T., and Jiang, H. (2022). Thermal field-actuated multifunctional double-emulsion droplet carriers: On-demand migration, core release and released particle focusing. Chem. Eng. J. 431, 134200. https://doi.org/10.1016/j.cej.2021.134200.
- de Wijs, K., Liu, C., Dusa, A., Vercruysse, D., Majeed, B., Tezcan, D.S., Blaszkiewicz, K., Loo, J., Lagae, L., Liu, J., et al. (2022). Microheater: material, design, fabrication, temperature control, and applications—a role in COVID-19. Biomed. Microdevices 24, 3. https://doi.org/10.1007/ s10544-021-00595-8.
- de Wijs, K., Liu, C., Dusa, A., Vercruysse, D., Majeed, B., Tezcan, D.S., Blaszkiewicz, K., Loo, J., and Lagae, L. (2017). Micro vapor bubble jet flow for safe and high-rate fluorescence-activated cell sorting. Lab Chip 17, 1287–1296. https://doi.org/10.1039/C6LC01560C.
- Bai, Y., Tian, J., Lin, Z., You, M., Liu, J., and Wang, X. (2020). Development of a high throughput micro-heater array with controllable temperature for each heating unit. Microsyst. Technol. 26, 787–792. https://doi.org/10.1007/s00542-019-04607-9.
- Lin, H., Yu, W., A. Sabet, K., Bogumil, M., Zhao, Y., Hambalek, J., Lin, S., Chandrasekaran, S., Garner, O., Di Carlo, D., and Emaminejad, S. (2022). Ferrobotic swarms enable accessible and adaptable automated viral testing. Nature 611, 570–577. https://doi.org/10.1038/s41586-022-05408-3.
- 82. Wu, M., Ouyang, Y., Wang, Z., Zhang, R., Huang, P.-H., Chen, C., Li, H., Li, P., Quinn, D., Dao, M., et al. (2017). Isolation of exosomes from whole blood by integrating acoustics and microfluidics. Proc. Natl. Acad. Sci. USA 114, 10584–10589. https://doi.org/10.1073/pnas.1709210114.
- Lomae, A., Preechakasedkit, P., Hanpanich, O., Ozer, T., Henry, C.S., Maruyama, A., Pasomsub, E., Phuphuakrat, A., Rengpipat, S., Vilaivan, T., et al. (2023). Label free electrochemical DNA biosensor for COVID-19 diagnosis. Talanta 253, 123992. https://doi.org/10.1016/j.talanta. 2022.123992.
- Cai, G., Yang, Z., Chen, Y.-C., Huang, Y., Liang, L., Feng, S., and Zhao, J. (2023). Magnetic Bead Manipulation in Microfluidic Chips for Biological Application. Cyborg Bionic Syst. 4, 0023. https://doi.org/10.34133/cbsystems.0023.
- Munaz, A., Shiddiky, M.J.A., and Nguyen, N.-T. (2018). Recent advances and current challenges in magnetophoresis based micro magnetofluidics. Biomicrofluidics 12, 031501. https://doi.org/10. 1063/1.5035388.

DeviceReview



- Yen, S.-H., Chin, P.-C., Hsu, J.-Y., and Lin, J.-L. (2022). Characterization of a Droplet Containing the Clustered Magnetic Beads Manipulation by Magnetically Actuated Chips. Micromachines 13, 1622. https://doi.org/ 10.3390/mi13101622.
- Cheng, Z., Wu, X., Cheng, J., and Liu, P. (2017). Microfluidic fluorescence-activated cell sorting (μFACS) chip with integrated piezoelectric actuators for low-cost mammalian cell enrichment. Microfluid Nanofluid 21, 9. https://doi.org/10.1007/s10404-017-1847-1.
- Zhang, Y.Y., and Xia, H.M. (2022). PZT actuator-controlled high-frequency microdroplet generation: Reducing the restrictions of channel size, fluid viscosity, and flow ratePZT. Sensor. Actuator. B Chem. 368, 132183. https://doi.org/10.1016/j.snb.2022.132183.
- Zhang, P., Chen, C., Su, X., Mai, J., Gu, Y., Tian, Z., Zhu, H., Zhong, Z., Fu, H., Yang, S., et al. (2020). Acoustic streaming vortices enable contactless, digital control of droplets. Sci. Adv. 6, eaba0606. https:// doi.org/10.1126/sciadv.aba0606.
- Godary, T., Binkley, B., Liu, Z., Awoyemi, O., Overby, A., Yuliantoro, H., Fike, B.J., Anderson, S., and Li, P. (2025). Acoustofluidics: Technology Advances and Applications from 2022 to 2024. Anal. Chem. 97, 6847– 6870. https://doi.org/10.1021/acs.analchem.4c06803.
- Wei, W., Wang, Y., Wang, Z., and Duan, X. (2023). Microscale acoustic streaming for biomedical and bioanalytical applications. TrAC, Trends Anal. Chem. 160, 116958. https://doi.org/10.1016/j. trac.2023.116958.
- Corato, E., Jakobsson, O., Qiu, W., Morita, T., and Augustsson, P. (2025).
 High-energy-density acoustofluidic device using a double-parabolic ultrasonic transducer. Phys. Rev. Appl. 23, 024031. https://doi.org/10.1103/PhysRevApplied.23.024031.
- Yadav, N., Giacomozzi, F., Cian, A., Giubertoni, D., and Lorenzelli, L. (2024). Enhancing the Deposition Rate and Uniformity in 3D Gold Microelectrode Arrays via Ultrasonic-Enhanced Template-Assisted Electrodeposition. Sensors 24, 1251. https://doi.org/10.3390/s24041251.
- Qiang, L., Vaddiraju, S., Rusling, J.F., and Papadimitrakopoulos, F. (2010). Highly sensitive and reusable Pt-black microfluidic electrodes for long-term electrochemical sensing. Biosens. Bioelectron. 26, 682–688. https://doi.org/10.1016/j.bios.2010.06.064.
- Brown, M.A., Zappitelli, K.M., Singh, L., Yuan, R.C., Bemrose, M., Brogden, V., Miller, D.J., Smear, M.C., Cogan, S.F., and Gardner, T.J. (2023).
 Direct laser writing of 3D electrodes on flexible substrates. Nat. Commun. 14, 3610. https://doi.org/10.1038/s41467-023-39152-7.
- Shi, S., Zhao, P., Yang, P., Zhao, L., Yi, J., Wang, Z., and Yu, S. (2025). Enhancing the Interfacial Adhesion of a Ductile Gold Electrode with PDMS Using an Interlocking Structure for Applications in Temperature Sensors. Nanomaterials 15, 1001. https://doi.org/10.3390/nano15131001.
- Wan, J., Zhou, S., Mea, H.J., Guo, Y., Ku, H., and Urbina, B.M. (2022). Emerging Roles of Microfluidics in Brain Research: From Cerebral Fluids Manipulation to Brain-on-a-Chip and Neuroelectronic Devices Engineering. Chem. Rev. 122, 7142–7181. https://doi.org/10.1021/acs.chemrev. 1c00480
- Park, Y., Franz, C.K., Ryu, H., Luan, H., Cotton, K.Y., Kim, J.U., Chung, T.S., Zhao, S., Vazquez-Guardado, A., Yang, D.S., et al. (2021). Three-dimensional, multifunctional neural interfaces for cortical spheroids and engineered assembloids. Sci. Adv. 7, eabf9153. https:// doi.org/10.1126/sciadv.abf9153.
- Cheng, X., Shen, Z., and Zhang, Y. (2024). Bioinspired 3D flexible devices and functional systems. Natl. Sci. Rev. 11, nwad314. https://doi.org/10. 1093/nsr/nwad314.
- 100. Chong, J., Sung, C., Nam, K.S., Kang, T., Kim, H., Lee, H., Park, H., Park, S., Kang, J., Holzreuter, M.A., et al. (2024). Innovative electrode and chip designs for transendothelial electrical resistance measurements in organs-on-chips. Lab Chip 24, 1121–1134. https://doi.org/10.1039/D3LC00901G.

- 101. Kulkarni, M.B., and Goel, S. (2022). Recent advancements in integrated microthermofluidic systems for biochemical and biomedical applications A review. Sensor Actuator Phys. 341, 113590. https://doi.org/10.1016/j.sna.2022.113590.
- 102. Epstein, A.K., Wong, T.-S., Belisle, R.A., Boggs, E.M., Aizenberg, J., Lin, Y., Genzer, J., Dickey, M.D., Lindner, E., Guzinski, M., et al. (2021). Electrically Controlled Neurochemical Delivery from Microelectrodes for Focal and Transient Modulation of Cellular Behavior. Biosensors 11, 348. https://doi.org/10.3390/bios11090348.
- 103. Jarmoshti, J., Siddique, A.-B., Rane, A., Hyler, A.R., Adair, S., Bauer, T.W., Swami, N.S., Chong, J., Sung, C., Nam, K.S., et al. (2025). On-Chip Integration of Impedance Cytometry for Inline Optimization of Dielectrophoretic Separations on Multiple Cellular Biophysical Metrics. ACS Sens. 10, 4116–4126. https://doi.org/10.1021/acssensors.5c00192
- Lin, Y., Genzer, J., and Dickey, M.D. (2020). Attributes, Fabrication, and Applications of Gallium-Based Liquid Metal Particles. Nature 7, 2000192. https://doi.org/10.1002/advs.202000192.
- 105. Chong, J., Sung, C., Nam, K.S., Kang, T., Kim, H., Lee, H., Park, H., Park, S., Kang, J., Holzreuter, M.A., et al. (2023). Highly conductive tissue-like hydrogel interface through template-directed assembly. Lab Chip 14, 2206. https://doi.org/10.1038/s41467-023-37948-1.
- 106. Lindner, E., Guzinski, M., Khan, T.A., and Pendley, B.D. (2019). Reference Electrodes with Ionic Liquid Salt Bridge: When Will These Innovative Novel Reference Electrodes Gain Broad Acceptance? ACS Sens. 4, 549–561. https://doi.org/10.1021/acssensors.8b01651.
- Epstein, A.K., Wong, T.-S., Belisle, R.A., Boggs, E.M., and Aizenberg, J. (2012). Liquid-infused structured surfaces with exceptional anti-biofouling performance. Nature 109, 13182–13187. https://doi.org/10.1073/pnas.1201973109.
- 108. Teekayupak, K., Lomae, A., Agir, I., Chuaypen, N., Dissayabutra, T., Henry, C.S., Chailapakul, O., Ozer, T., and Ruecha, N. (2023). Large-scale fabrication of ion-selective electrodes for simultaneous detection of Na +, K+, and Ca2+ in biofluids using a smartphone-based potentiometric sensing platform. Mikrochim. Acta 190, 237. https://doi.org/10.1007/s00604-023-05818-8.
- Ozer, T., Agir, I., and Henry, C.S. (2022). Low-cost Internet of Things (IoT)-enabled a wireless wearable device for detecting potassium ions at the point of care. Sensor. Actuator. B Chem. 365, 131961. https://doi.org/10.1016/i.snb.2022.131961.
- 110. Xiao, Z., Li, W., Moon, H., Roell, G.W., Chen, Y., and Tang, Y.J. (2023). Generative Artificial Intelligence GPT-4 Accelerates Knowledge Mining and Machine Learning for Synthetic Biology. ACS Synth. Biol. 12, 2973–2982. https://doi.org/10.1021/acssynbio.3c00310.
- Blocklove, J., Garg, S., Karri, R., and Pearce, H. (2023). Chip-Chat: Challenges and Opportunities in Conversational Hardware Design. In 2023 ACM/IEEE 5th Workshop on Machine Learning for CAD (MLCAD), pp. 1–6. https://doi.org/10.1109/MLCAD58807.2023.10299874.
- 112. Kundacina, I., Kundacina, O., Miskovic, D., Radonic, V., Liu, C., Kundacina, I., Kundacina, O., Miskovic, D., and Radonic, V. (2025). Advancing microfluidic design with machine learning: a Bayesian optimization approach. Lab Chip 25, 657–672. https://doi.org/10.1039/D4LC00872C.
- 113. Homayouni-Amlashi, A., Koebel, L., Lefevre, A., Mohand-Ousaid, A., and Bolopion, A. (2024). Topology optimization of the electrodes in dielectrophoresis-based devices. Comput. Struct. 301, 107444. https://doi.org/ 10.1016/j.compstruc.2024.107444.
- Liu, R., Wang, N., Asmare, N., and Sarioglu, A.F. (2018). Scaling codemultiplexed electrode networks for distributed Coulter detection in microfluidics. Biosens. Bioelectron. 120, 30–39. https://doi.org/10.1016/j. bios.2018.07.075.
- 115. Clausen, C., Skands, G., Bertelsen, C., and Svendsen, W. (2014). Coplanar Electrode Layout Optimized for Increased Sensitivity for

Please cite this article in press as: Shen et al., Designing and integrating microfluidic electrodes for biosensing and micromanipulation, Device (2025), https://doi.org/10.1016/j.device.2025.100964





- Electrical Impedance Spectroscopy. Micromachines 6, 110–120. https://doi.org/10.3390/mi6010110.
- 116. Guo, K., Song, Z., Zhou, J., Shen, B., Yan, B., Gu, Z., and Wang, H. (2024). An artificial intelligence-assisted digital microfluidic system for multistate droplet control. Microsyst. Nanoeng. 10, 138. https://doi.org/10.1038/s41378-024-00775-5.
- 117. Liang, T.-C., Chang, Y.-C., Zhong, Z., Bigdeli, Y., Ho, T.-Y., Chakrabarty, K., and Fair, R. (2024). Dynamic Adaptation Using Deep Reinforcement Learning for Digital Microfluidic Biochips. ACM Trans. Des. Autom. Electron. Syst. 29, 1–24. https://doi.org/10.1145/3633458.
- 118. Kullberg, J., Sanchez, D., Mitchell, B., Munro, T., and Egbert, P. (2023). Using Recurrent Neural Networks to Reconstruct Tem-

- peratures from Simulated Fluorescent Data for Use in Bio-microfluidics. Int. J. Thermophys. *44*, 164. https://doi.org/10.1007/s10765-023-03277-0.
- 119. Sun, R., Jeong, H., Zhao, J., Gou, Y., Sauret, E., Li, Z., and Gu, Y. (2024). A physics-informed neural network framework for multi-physics coupling microfluidic problems. Comput. Fluids 284, 106421. https://doi.org/10. 1016/j.compfluid.2024.106421.
- Schmidt, F., González-Gómez, C.D., Sulliger, M., Ruiz-Reina, E., Rica-Alarcón, R.A., Ortega Arroyo, J., and Quidant, R. (2025). Three-dimensional optofluidic control using reconfigurable thermal barriers. Nat. Photon., 1–7. https://doi.org/10.1038/s41566-025-01731-z.